Int J Fract (2007) 143:41–78
DOI 10.1007/s10704-007-9050-0

ORIGINAL PAPER

Multi-scale interaction potentials ($F - r$) for describing fracture of brittle disordered materials like cement and concrete

Jan G. M. van Mier

Received: 16 June 2006 / Accepted: 3 January 2007 / Published online: 21 February 2007

Abstract Fracture processes in brittle disordered materials like many geo-materials (rock, ice, concrete, cement, etc.) are a trade off between local stress concentrations caused by the heterogeneity of such materials, and local strength. At those locations where the ratio between stress and strength exceeds a critical threshold value, cracking may initiate. Depending on the size of the cracks they can be arrested by stronger and stiffer elements in the structure of the material, or they will propagate and become critical. Critical cracks lead to localisation of deformations and to softening. In currently popular cohesive crack models still some continuum ideas remain, namely the notion of stress, whereas the localisation of deformations is handeled correctly by means of displacements. During softening the macro-crack traverses the specimen's cross-section, thereby gradually decreasing the effective load-carrying area. This growth process is affected both by structure (specimen) size and boundary conditions, and a better description of softening may be achieved by using load and displacement as state variables. In this paper, a new method of modelling fracture is proposed by using fracture potentials ($F - r$ relations) at various observation scales, from atomistic and molecular to macroscopic. The virtual material can be interpreted as being built up from spherical elements; the fracture potential describes the interactions between the spheres. Since the spherical elements interact at their contacts-points only, a force-separation law (F–r) suffices. Size/scale effects are dealt with directly in the F–r relation; size/scale effects on strength are merely a special point in the entire description and do not require a separate law.

Keywords Cementitious materials · Cement · Concrete · Disorder · Brittleness · Ductility · Material · Structure · Interaction potential (F–r) · Multi-scale

J. G. M. van Mier (✉)
Materials Research Center and Department of Civil, Environmental and Geomatics Engineering, Institute for Building Materials, ETH Zürich, 8093 Zurich, Switzerland
e-mail: jvanmier@ethz.ch

1 Introduction

Concrete and ice, sandstone and other types of rock all have rather complex material structures. Most of these materials are built-up from different types of minerals, where the geometry of the grains may be quite regular (for example hexagonal structures of basalt, fresh-water ice) or tremendously irregular (granite, salt-water ice, cement). A full understanding of fracture phenomena in these materials has not been achieved. On a global scale cohesive crack models have been embraced by engineers to model fracture. However, since structural effects (i.e., effects deriving from

the boundaries of the considered specimen/structure (construction) such as boundary rotation effects in uniaxial tension, size effects in uniaxial tension and uniaxial compression, and boundary friction effects in uniaxial compression, see Van Mier (1997) for an overview influence the softening behaviour, the result from experiments can not be used directly as material property. In spite of this, softening relations are commonly used, and only few consider the material/structural interactions that take place. One problem is that the critical localized macro-crack (or shear band in compression) grows gradually through a specimen's cross-section, thereby gradually decreasing the effective load-carrying area. Stress is thereby not a correct state variable, and should be replaced by an alternative. Several years ago Hillerborg and co-workers (see Hillerborg et al. 1976) proposed to replace strain in the softening regime by displacement; we are now more or less facing the problem of having to drop stress as state variable as well.

In this paper, it is tried to propose a new road to solve the problem. The solution is sought in multi-scale interaction potentials that effectively describe the interaction between two particles in contact. The particles can be atoms, or larger entities like grains or even macroscopic balls; essential is that their interaction is confined to a single point. At each size-scale the interaction potential may be caused by various physical mechanisms, like direct atomic binding, capillary water forces at the level of cement, sand or clay particles, etc. Structures can be interpreted as composed of many particles in contact, and the interaction laws in terms of force and displacement form the constitutive equation. After a review of the material structure of cement and concrete at various size/scale levels, attention turns towards primitive lattice models that can be used for describing fracture of heterogeneous materials from a given size/scale upwards. Applying lattices from the atomistic scale upwards leads to unsolvable computational problems, and at this point the afore-mentioned interaction potentials are introduced. Next the papers turns to size-scale effects, demonstrating that scaling of strength is just the peculiar outcome of crack processes at one scale level smaller than the observed load–displacement diagram. In principle these crack processes can be controlled by the heterogeneity of the material under consideration. The strength of the material must be understood as the point where pre-critical cracking turns into a critical crack that cannot be arrested by stronger and stiffer elements in the material structure anymore. In other words, that arrest mechanism has been exhausted. When considering cement and concrete, different physical mechanisms affect the interaction between particles at different size-scales. Basically the interaction potential at any given size-scale can be computed on the basis of knowledge of the respective physical processes at the considered size-scale level. In the paper, it is attempted to get some grip on these matters. Finally, some open questions and problems are summarised.

2 Disordered material structures

Material structures are usually not very regular, and disorder is rule rather than exception. First of all disorder can be observed in the material structure, sometimes also referred to using terms as texture, fabric, etc. This is pure geometry: grains, pores, grain boundaries, platelets, fibres, etcetera, are recognized in the material structure as patches with distinct properties from neighbouring areas.

Starting at the atomic level, the only structures to have no disorder are pure crystal lattices. Atoms are arranged in regular arrays in 2- or 3-dimensions. Two-fold, three-fold, four-fold, or six-fold symmetries have all been observed in nature, whereas five-fold symmetry exists also, but then in somewhat more disordered arrangements and are usually referred to as quasi-crystals. Examples of regular ordering of atoms are the face-centered cubic lattice and the hexagonal close-packed lattice. If crystals are arranged in neighbouring patches of material, then at larger scales, usually referred to as micro- or meso-scale disorder is created at the boundaries where the respective material patches (or grains) meet. Along the boundaries between patches built up from different crystals there exists a certain mismatch, and so-called grain-boundaries with quite distinct properties appear. In the afore-mentioned hexagonal basalt and ice structures, grain boundaries are arranged along regular repeating patterns (in one cross-section). This is not necessarily always so. In granite, salt-water-ice,

various metals and ceramics, the grains have rather random shapes, and the material structure becomes very irregular. Again, other materials like concrete, fibre reinforced composites have a certain regularity caused by the added phase, such as aggregates and fibres. Aggregates have almost similar dimensions in three orthogonal directions, whereas fibres are elongated in a single direction. Platelets, the third type of inclusion, have two almost similar dimensions and a third, much smaller, dimension. As an example the structure of cement and concrete at nano-, micro,- and meso-scale is shown in Fig. 1. In this figure also a more correct interpretation of a continuum is shown. Often the macroscale is referred to as a continuum where no internal structure is recognized. However, a continuum has an abstract (mathematical) internal structure as suggested in Fig. 1, and can actually be applied at any of the observational scales drawn above the box representing the continuum. The prime task is to see whether a continuum representation of physical processes taking place at any of the shown size/scale levels (leading often to nonlinear 'material behaviour') can be represented as an 'averaged' process as any continuum representation implies. It is quite obvious that such attempts lead to complications for discrete localized fracture, where large displacement jumps will occur at the scale of the considered material specimen (or structure).

Returning to the structure of cement and concrete, at the **meso-scale** (here: *mm*-scale) individual aggregates are visible in concrete (and mortar; a useless distinction made solely based on the fact that the aggregates are smaller than in concrete). This particular image shows the structure of a weak concrete ($f_c = 10\,\text{MPa}$). The white specs are unhydrated cement kernels, the small gray particles represent hydrated cement and black is porosity. Large aggregates are observed, which appear to have some internal structure as well. In the meso-level representation of concrete the aggregates are usually modelled as an isotropic continuum. Similarly, for the cement matrix a continuum representation is used too, assuming that the size of the hydrated and un-hydrated cement and the small scale porosity is small in comparison to the matrix dimensions. This is debatable, especially at places where aggregates come close together and a thin ribbon of cement is inserted between the aggregates. The third phase commonly distinguished in meso-models of concrete is the interfacial transition zone (ITZ) which has been identified as a zone of rather large porosity enveloping the aggregates (Scrivener 1989). There is some debate about the validity of these measurements, since meso-level material structures like the one depicted in Fig. 1 do not really show a well distributed porosity in the ITZ, and the conclusion drawn by Scrivener might have been the result of the specific way of averaging microstructural information along the circumference of large aggregates. Diamond and Huang (1998) debated the result using 2D SEM images as 'proof' for the erroneous idea of Scrivener. However, drawing conclusions about a 3D microstructure based on 2D images must be done with extreme caution since 3D information is easily misinterpreted, or simply goes un-noticed. The best solution is to gather 3D material structural information, which can for example be done using X-ray tomography, see for example in Trtik et al. (2005a).

At the **micro-scale**, polished sections indicate the structure shown in Fig. 1 (the scale is μm). In this image rather good quality cement is shown, with un-hydrated cement as white, a dark gray zone enveloping the un-hydrated grains, and black specs that indicate porosity. There are shades of gray that are often assumed to be the result of two different hydration products: inner and outer Calcium Silicate Hydrates (CSH). On first sight there is not much difference between the micrometer structure and the millimeter structure and in both cases a very heterogeneous disordered material structure is found. The aggregates in normal concrete and the un-hydrated cement kernels both have a rather large stiffness in comparison to the surrounding matrix, and are usually stronger as well.

Finally, zooming in a further three orders of magnitude shows the structure of the hydration products themselves at the **molecular-scale** (nano-scale). The molecular structure of CSH is still under debate, and direct observations using TEM are tedious and very difficult in view of problems encountered in sample preparation. Pellenq and Van Damme (2004) and Gmira et al. (2004) published some results from TEM observations. A model for the molecular structure of CSH was proposed, in which water plays an important role as

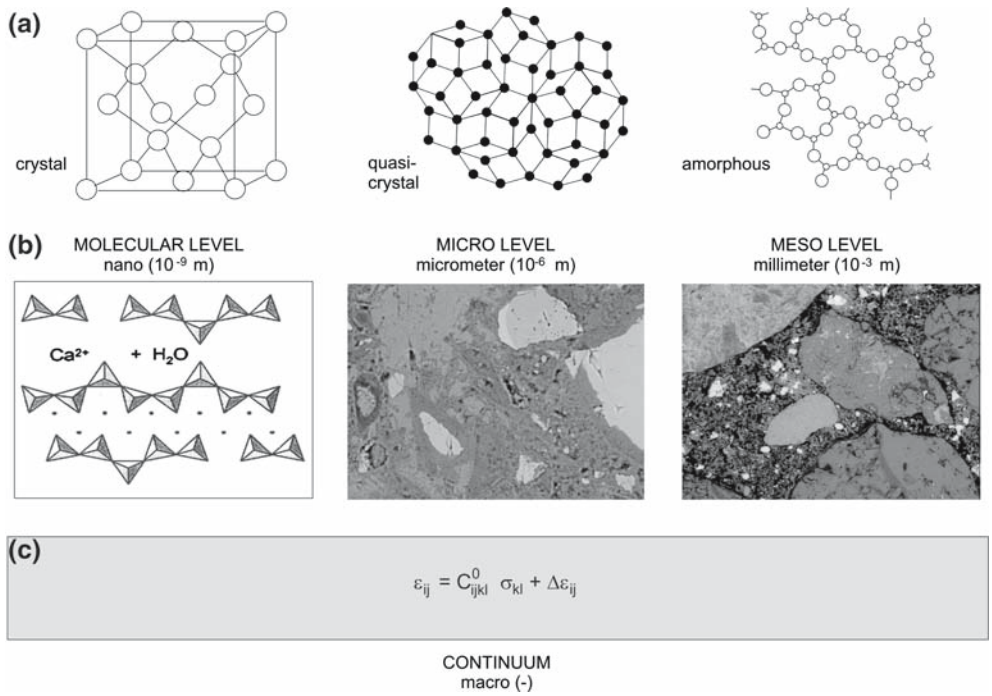

Fig. 1 (**a**) Possible atomistic material structures (crystals, quasi-crystals and amorphous), (**b**) material structures at nano/micro/meso-scale for cement and concrete, and (**c**) continuum interpretation, where the only internal structure left is the mathematical formulation. The concrete meso-structure was kindly supplied by Dr. A.S. Elkadi, see also Elkadi (2005) for more details on the mixture composition

well (this will be discussed further on in this paper, see Sect. 6). The image of the molecular structure in Fig. 1 is schematic, and only is shown to indicate what can be expected at this level. Distance between layers in the CSH structure is estimated at 1.5 nm (Pellenq and Van Damme 2004). Gatty et al. (2001) observed a rather heterogeneous structure of CSH using TEM: nano-crystalline and 'meso-scale' ordered regions within an amorphous matrix were found, where it was suggested that the nano-crystalline phase has a tobermorite-like structure and the mesoscale order reflects modulations in water content. The use of the term 'mesoscale' is relative to the observational scale in the order of *nm*, and is thus different from the use of the word meso-level in this paper. The results by Gatty et al. suggest that heterogeneity and disorder continues to very small observational scales for cement and concrete. The observational scales become in fact so small that one is dealing with molecules.

The different elements in a certain material structure have distinct properties, such as the stiffness of the bonds, and/or the strength may vary, as can the 'toughness' vary. Toughness must be understood as a size-dependent property, since it may change from brittle to ductile depending on the dimensional properties of the material structure, and the structure (specimen/construction) as a whole (see the more extensive discussion in Sect. 7).

The main issue here is that the different material structures lead to different internal stress distributions, caused by E-mismatch between the different phases, porosity, shape and size of microstructural elements, and so on. Irrespective of the type of external loading, the internal stress-field is not uniform. If the stress variations are limited, and the size of the microstructure is small compared to the overall structure size, one might decide to adopt averaging procedures, and model the material as a continuum. This is valid then for the microstructure in the 'stationary' stage where no damage in

the form of cracks appears due to some sort of loading. The reason for this remark is that when cracks become large, the specimen size becomes an issue. This is well described using fracture mechanics approaches.

The example given here is for cement and concrete material structures. Other materials display heterogeneity at different levels of observations as well, and cannot be discarded when observational scales decrease. Most dramatic is probably the glass studied by Célarié et al. (2003), where the amorphous structure of the material seems to have a distinct effect on the fracture process.

3 Simple lattice approach

In statistical physics, for example in lattice models or cellular automata, randomness of material properties due to distinct elements in the materials microstructure is incorporated through a statistical distribution of lattice properties such as stiffness, strength threshold, and so on (see for example Mourkazel and Duxbury 1994; Duxbury et al. 1995; Hansen 1991; Herrmann et al. 1989; Herrmann and Roux 1990; Alava et al. 2006 and many others). It seems, however, that such approaches might miss some of the relevant detail of real micro-structures as described in the previous section, and therefore, a procedure where the actual material structure is mapped on a lattice, cellular automaton, or finite element mesh seems more appropriate (e.g., Roelfstra et al. 1985; Stankowski 1990; Schlangen and Van Mier 1992; Schlangen 1993; Wang et al. 1993; Arslan et al. 1995; Bolander et al. 1996). In Fig. 2 some examples of possible material representations are shown, each time showing better agreement with the real meso-structure of concrete (note: in principle lattices, finite element models and cellular automata can be used at any scale level, as long as the adopted mechanics/physics is still valid). Lattices with either quenched disorder (i.e., disorder introduced before the breakdown process starts) or annealed disorder (no disorder at the beginning of the breakdown process, but introduced through a stochastic breaking algorithm) are the general approaches in statistical physics. However, when for a material more information is available about its microstructure one might as well try incorporating this information directly in the model. In Fig. 2a the lattice model of Burt and Dougill (1977) is shown, where the actual disorder comes from the connectivity of the elements and the different beam lengths. Heyden (2000) developed a lattice model for cellulose fibre fluff where the lattice elements may overlap, and are connected by various types of springs at the location of these overlaps. Mourkazel and Herrmann (1992) developed another type of random lattice, with varying element lengths, which has been quite useful in some of our own analyses. The problem here, and also in the statistical approach, is that somehow the distribution of either element length or material disorder distribution must be matched to distributions of salient properties of the material constituents (see Chiaia et al. 1997; Van Mier et al. 1997, 2002), which is certainly not an easy task in the case of concrete and other types of geo-materials. Inverse identification might be the way out, but this will work only if the parameters all have a physical basis. In the model of Vonk (1992) computational convenience was the reason to operate with hexagonal aggregates that were randomly distorted into polygons (Fig. 2b). The advantage here is that the distribution of strong/stiff and weak/soft patches as found in real mortar and concrete is included in the model, but the geometry is far from the real one. The use of circular (in 2D) or spherical aggregates (in 3D) by Schlangen and Van Mier (1992) and Lilliu and Van Mier (2003), respectively (Fig. 2c), avoids the stress-concentrations caused by aggregate angularity in Vonk's model, but again, the used 3-phase representation is not completely according the real concrete material structure (see Fig. 1b (meso)).

The large advantage of the method developed by Schlangen and Van Mier (1992) and that led to Schlangen's thesis (1993) is that the particle structure and lattice are generated independent of each other. The lattice structure is the computational 'back-bone', whereas in Vonk's model, for example, or the 'numerical concrete' model by Roelfstra et al. (1985) the two- or three-dimensional finite elements have to be fitted to the complex material structure, which is particularly tedious in three dimensions. Independent generation of lattice and particle structure also opens the way to

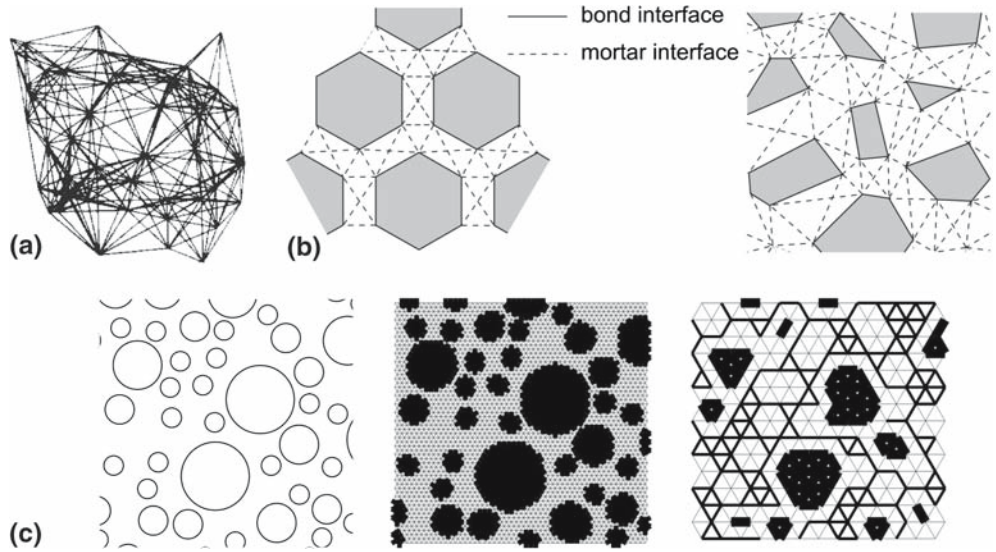

Fig. 2 Examples of computer generated material structure intended to mimic the structure of concrete at the meso-level: (**a**) Burt and Dougill (1977), (**b**) Vonk et al. (1991) and (**c**) Schlangen and Van Mier (1992)

use real aggregate shapes, as was demonstrated by Schlangen and Garboczi (1997), in a way similar to the generation of computational cement hydration models pioneered at NIST by Bentz et al. (1994).

The mechanics of lattice models is relatively simple: the basic need is a finite element programme capable of linear elastic truss or frame analysis. The truss analysis is straightforward, the beam analysis requires Timoshenko beams (as mentioned by Ince et al. 2003), rather than the originally proposed Euler-Bernoulli beams used by Schlangen and Van Mier (1992), which is due to the rather stubby shape of the beams. The stubbiness of the beams is caused by fitting of the elastic properties of a lattice to real (global) concrete elastic properties, see Schlangen (1993). The use of linear elements simplifies the generation of three-dimensional lattice structures with or without material structure. Important is to choose the lattice elements sufficiently small in comparison to the smallest element in the projected particle structure. This is quite essential since otherwise rather large amount of carefully gathered information on the microstructure is lost in a too coarse discretization (see Fig. 2c: particle overlay with fine and coarse lattice affects the shape of the particles).

The key factor in a lattice model is the selection of a failure criterion for the beams. The choice of a failure criterion seems directly related to the scale of discretization, i.e., nano-, micro-, or meso-scale in cement and concrete, see Fig. 1b. From the chosen discretization scale it is possible to calculate structures of larger dimensions; going to smaller scales is prohibited. In most meso-models it is assumed that the lattice elements break upon reaching a certain stress level, which can be computed on the basis of several assumptions. For example, most straightforward is the normal stress criterion, where the normal force in the lattice is used to compute an effective lattice stress, which is compared to the critical threshold depending on the location in the material structure, following

$$\sigma > \sigma_{\text{eff}} = \frac{F}{A}. \tag{1}$$

Upon reaching the critical stress level, the considered lattice element is simply removed, and the next linear analysis is carried out on the lattice having $N - 1$ elements. This process continues until the entire lattice fails. Computational problems arrive when more and more detail is included in the model, which causes an enormous increase in the number of lattice elements. Ince et al. (2003), as well as others, proposed to use a softening relation for failure of the lattice elements in order to

use coarser lattices. The new problem introduced is that an iterative procedure is needed to solve the equations, which may lead to similar computational problems as faced in higher order continua. Mesh-dependency is not an important issue in lattice analyses since a material length scale is included by directly incorporating material heterogeneity, which is often the dominating factor. Lattice analysis can only be used for analyzing structures larger than the defined model-scale. The parameters, like the fracture law, depend also on the defined model-scale. The fracture law thus contains (un-known) information from (un-known or discarded) phenomena at lower scales, and is thus per definition phenomenological. Completely ab-initio analysis from quantum-mechanical and/or atomic principles is possible for very small material volumes only, which are rather distant (i.e., simply too small) for the cement and concrete considered in this paper.

When a particle structure like the one shown in Fig. 2c is mapped onto the lattice material properties of three material phases must be specified, namely, the tensile strength and the Young's modulus of aggregate, matrix and interface elements. The largest problems are encountered for the ITZ. Zimbelmann (1985) showed that the tensile strength of the interface is relatively low, in most cases not exceeding 1 MPa. The tensile strength of cement matrix and aggregate particles can be a factor 5–10 higher. Thus, the weak link is the interface between aggregate and matrix (at least in normal concrete, the situation changes for concretes containing low strength highly porous aggregates, that may actually have a stronger interfacial strength, see Vervuurt 1997). The Young's moduli, at least those of matrix and interface, play a lesser role, as shown in Van Mier and Veruurt (1997). This result is quite similar to results obtained by He and Hutchinson (1989) who in addition analyzed the influence of the incidence angle of the crack.

The magnitude of the breaking forces of lattice elements are dependent on the scale of discretization. One might envision hierarchical lattices, like the model proposed by Breysse (1991), where each element consists of a network of smaller elements, each with their own breaking threshold. Basically these are attempts to model the material at multiple scales. Multiple-scale modelling has developed into an active research field in the past years. A hierarchy built into a lattice might result in a gradual failure of a lattice element at large scale, caused by microfracture processes at lower hierarchical levels. This could be interpreted as using a softening breaking law, where the softening is the global response of all micro-fracture events. This may help to circumvent brittleness problems encountered in lattice analyses, as was shown by Ince et al. (2003). We will return to these matters in Sect. 7.

We will not dwell any further on lattice analyses, other than saying that the method is very effective, simple and straightforward. The laboratory samples as tested in real experiments can be modelled as they are, including the boundary conditions used in the experiments. This latter point is of great importance in view of the significant influence of the boundary conditions on the macroscopic crack growth during global softening. Thus, rather than assuming that the outcome of a laboratory experiment is a property of the material, the idea is not to make any assumptions at all and *to consider the experiments as a test on a small-scale structure*. Although this idea was launched in 1984 (see Van Mier 1984, 1986) and actually makes sense in view of boundary condition effects during global softening in uniaxial compression (Van Mier 1984; Kotsovos 1983; Vonk 1992) and in uniaxial tension tests (Van Mier et al. 1994), it has not gained general acceptance. Especially the continued—and hitherto un-successful—search in the concrete fracture mechanics community for a standard test for measuring the softening properties under tension (and other loading cases) underscores this remark. Test methods employing complicated three-actuator loading devices to overcome secondary bending due to non-uniform macrocrack growth in uniaxial tension tests (Carpinteri and Ferro 1994) or more simple devices using a manual gear (Akita et al. 2003) lead to rather uniformly distributed deformations around the specimen's circumference. At the same time quite distinct crack densities develop, and higher fracture energies are obtained compared to the cases where the specimen boundaries are either freely rotating or fully fixed against rotation, see in Van Mier et al. (1994). In addition to that, there is a distinct size effect on fracture energy (Trunk

2000; Van Vliet 2000), which makes it difficult to decide which size to choose in the standard test. Thus, a suitable size/scale-effect model that would describe structural scaling effects must be found as well, and should form an integral part of the proposed test method. We will return to size/scale effects in Sect. 4, which is probably the single most important issue that must be considered in fracture mechanics of concrete. To the author's opinion, it is better to accept that softening is *not* a material property; instead softening should be interpreted as a combined material/structural property. This can be recognized in the four-stage fracture model proposed in Van Mier (2004), in which both material effects and structural effects (in the fracture mechanics formulation) are accounted for. In this approach softening is described by means of a bridged-crack model, where the growth of the macrocrack is modelled using classical fracture mechanics principles (K_{Ic}-criterion), with a bridging stress resembling the tail of the softening diagram only.

An example of the outcome of a (2D) lattice analysis where different particle densities were used is shown in Fig. 3. These results were published in Prado and Van Mier (2003), and are of importance for the discussion to follow. The particle distributions for these analyses were computer-generated using the SPACE model developed by Stroeven (1999). The three analyses shown are one case with a low particle density (35% before lattice overlay), a second with extreme high particle density (83% before lattice overlay), and a third with intermediate particle density of 51%. Since all particles are enclosed by an ITZ of a single beam length, the low density case can be characterized by aggregates 'swimming' in a cement matrix with non-connected ligaments of matrix material between the ITZ's. In the high density case, it is easy to see that all ITZ's are connected, and the amount of matrix material has decreased substantial. In other words, at low density the matrix material is the percolating phase, at high density the ITZ-phase. Considering that the strength ratio is 10:5:1.25 for the aggregate, matrix and ITZ-phases, the global strength of the low particle density case (Fig. 3a) is determined by the matrix strength, and higher compared to the high particle density case where the global strength depends on the ITZ strength (Fig. 3c). Similar results were observed in 2D and 3D by Lilliu and Van Mier (2003), and earlier using quenched disorder in 2D and 3D models by Duxbury et al. (1995) and Mourkazel and Duxbury (1994). The result is actually quite trivial for the extremes, but the behaviour at intermediate particle densities is more complex. The important difference is in the pre-peak micro-cracking. Here the global strength of the concrete is decided, which has consequences for scaling of fracture strength, as will be discussed in Sect. 4.

Returning to Fig. 3, a set of basic observations can be made that are important for the discussion in the remainder of this paper.

(i) The load–displacement diagrams show that with increasing particle density the maximum strength decreases, which is caused by a diminishing hardening regime.
(ii) Small aggregate quantities lead to discontinuous bond zones and the possibility to the formation of distributed microcracking in a band. The 'crack-band' is very manifest at small densities (Fig. 3a) and disappears at large densities (Fig. 3c).
(iii) During stages (B) in the load–displacement diagrams, the macro-crack traverses the specimen's cross-section. This is in agreement with experimental observations. Cracking seems to be limited to occur in the immediate vicinity of the main macro-crack; no further microcracking appears to develop farther away from the main crack.
(iv) The green, yellow and red colour shades in the crack diagrams show the stress-concentration in the specimens. Red (dark gray in B/W printing) indicates a higher stress than average, whereas light yellow/green indicates a lower than average stress. In the path of the macro-crack high stress concentrations appear, which are a sign of bridging activity.

Thus, the post-peak behaviour shows macro-crack propagation and bridging. As mentioned, bridging is visible as the dark-coloured (red) stress concentrations along the main macrocrack in the images of Fig. 3. From experiments bridging in the form of overlapping cracks is known for concrete for a number of years. Figure 4 shows an example where two overlapping crack tips meet and join together

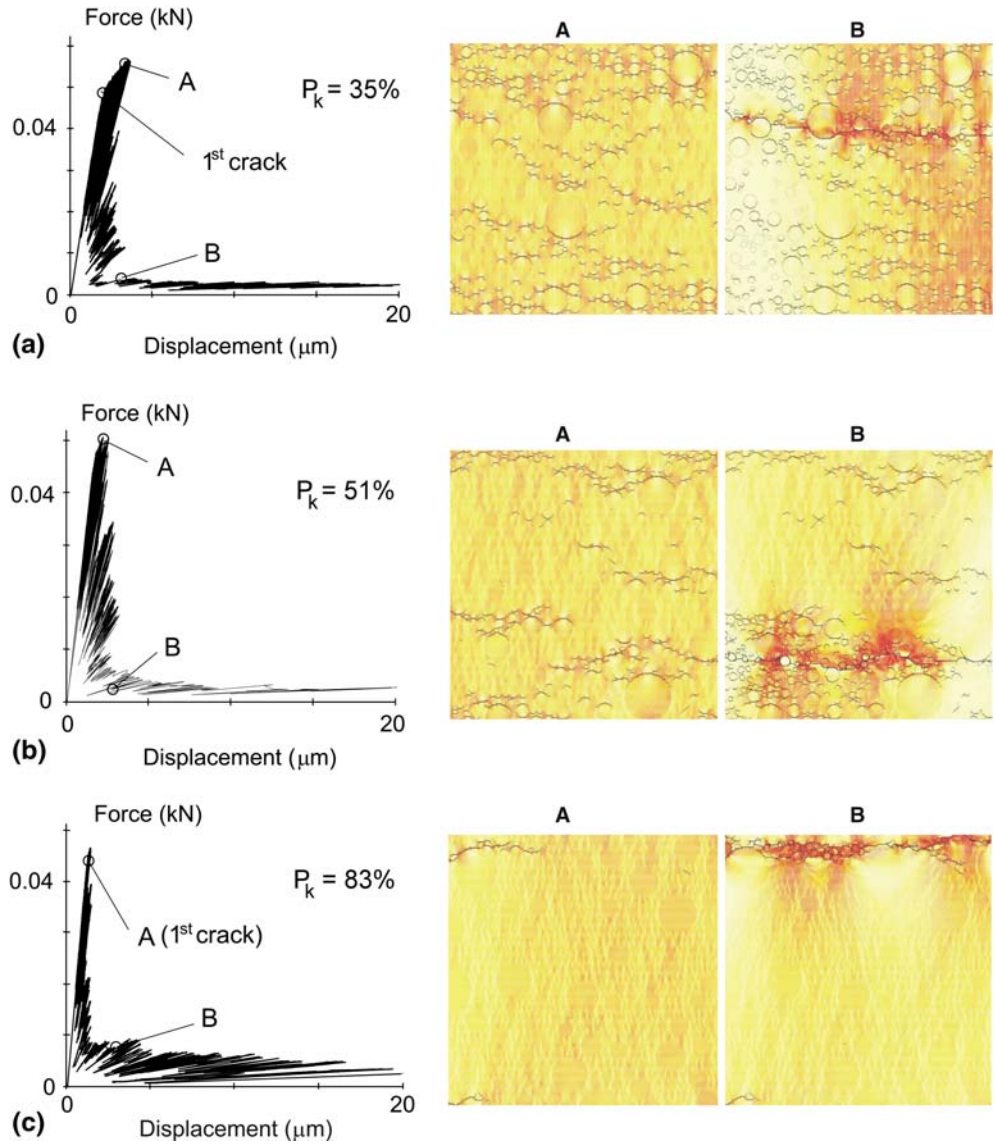

Fig. 3 Effect of particle density on fracture of concrete under uniaxial tension: results from numerical lattice simulations, after Prado and Van Mier (2003). In (**a**) the load–displacement diagram and the fracture patterns at peak-load and at 25 μm displacement are shown for aggregate density $P_k = 35\%$, in (**b**) for an aggregate density of 51%, and in (**c**) for $P_k = 83\%$

in the wake of one of the tips. The growth of the active crack tip is accompanied by similar crack overlaps at smaller scales, indicating that a hierarchical fracture process occurs in concrete.

This overlap crack mechanism (or 'hand-shake crack') appears in many different materials, such as rock, ceramics, ice, asphalt, dental material, and recently it was suggested that the same holds for glass. Two approaching crack tips avoid each other when they approach head on (Simha et al. 1986), and the hand-shake crack that develops has been known for long time in the afore-mentioned materials, see for example in Sempere and Macdonald (1986). Relating this crack bridging mechanism to the carrying capacity of cracked material, i.e., concrete, was done by Van Mier (1991a,b) for the first

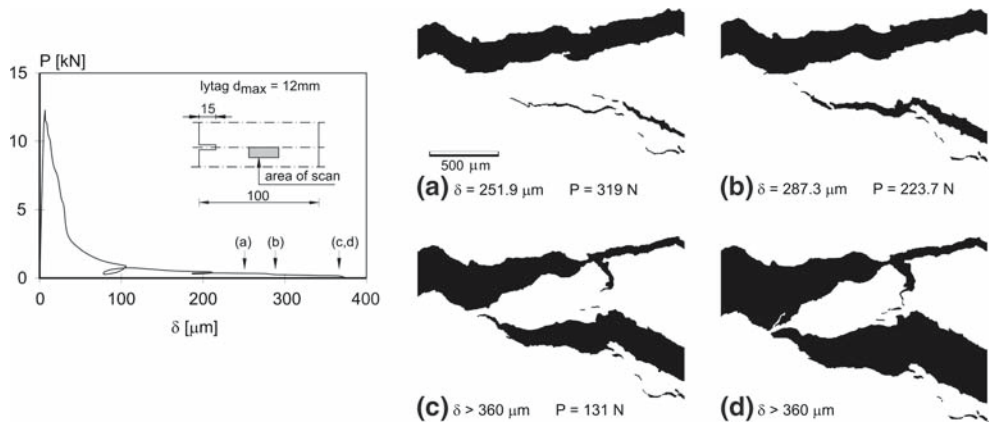

Fig. 4 Four stages of failure of the ligament between two overlapping crack tips, after Van Mier (1991b). The final cracking involves flexural cracking in the final ligament (**c**) as well as chip formation (**d**). Note the abundant micro-cracking in the neighbourhood of the main crack in stages (**a**) and (**b**)

time. Of course the mechanism is "assisted" by the heterogeneity of the material, and concrete is in this respect an interesting material due to its rather coarse heterogeneity, which helps to detect said phenomena in lab-sized specimens (scale 10^{-2} m). We will not dwell upon these matters any longer here since they have been explained in minute detail in Van Mier (1997). Wake bridging is important in the tail of the diagram, and the crack overlap mechanism seems basic to stress-transfer in that regime. In other materials, for instance certain type of ceramics, frictional effects seem to play a role as well, for example the frictional pull-out of whiskers from a matrix as described by Steinbrech et al. (1991) and Swanson et al. (1987).

The demonstration of pre-peak micro-cracking is much more difficult owing to the extreme small dimensions (in particular the width) of microcracks. Direct viewing has been hampered by additional damage done during sample preparation, and the only 'proof' of pre-peak cracking is derived from AE monitoring, e.g., Wissing (1988) and Otsuka et al. (1998). The latter tests also reveal that the width of the band where acoustic emission is monitored is gradually narrowing indicating that the analyses of Fig. 3 might actually be quite close to reality.

Using a materials science approach has helped to unravel the mechanisms underlying softening, and it is clear that combined structural/material behaviour is observed. Structural effects play a minor role in the pre-peak regime when microcracking is arrested by the material structure itself. The material structural effects are also quite obvious in the tail of the softening diagram, in the form of hand-shake cracks with intact ligaments in-between, or by means of frictional pull-out of particles or fibres in, for example, ceramics and/or fibre reinforced materials. Structural effects are most pronounced during the macro-crack growth where classical fracture mechanics principles should be used to explain specimen size and boundary condition related effects. The influence of boundary conditions, for example, the type of support used in beam tests (with or without friction), the rotations allowed in uniaxial tension tests (freely rotating or rotations completely prohibited during the entire test) have a significant effect on the failure mechanisms, as demonstrated on many occasions in the past (see in Van Mier 1997 for a complete overview) and to the author's opinion cannot be ignored in fracture analyses of any type of material. The structural effects, for example in SEN and DEN shear beams, and in uniaxial compression tests can be readily analyzed by means of lattice type models and other micro-mechanical models, see for example in Schlangen (1993), Vonk (1992), and D'Addetta (2004).

Finally, some remarks on the computational effort needed in micromechanical models in materials science. Atomistic simulations appear to follow the famous Moore law, which predicts a linear

increase in time of the log number of atoms considered in a simulation; see for example in Kalia (2004). Lattice analyses with the beam model lead to a similar increase in computational possibilities. The number of beams in the early models employed by Schlangen and Van Mier (1992) was in the order or 10^3. The increasing speed of processors, the employment of parallel computers using dedicated parallel solvers (e.g., the solver developed by Lingen 2000, used in Lilliu and Van Mier 2003) or clever methods to optimize the matrix inversion (Nukala and Simunovic 2005) allows to analyze problems in the order of 10^5–10^7 beam elements at present, i.e., a factor 10^3–10^4 larger in almost 15 years. Although this increase is impressive, it prohibits simulating samples at laboratory scale or larger, even so more when all kinds of nonlinear processes are included, like in cement and concrete, drying, hydration, etc. Therefore, there is need for a faster approach that is capable of including these mechanisms in a simple and straightforward manner, without having to resort to full-scale (numerical) atomistic or micromechanical analyses.

In conclusion, micromechanical analysis of materials is a useful tool to qualitatively assess *failure mechanisms*, which, as should be clearly understood, MUST always be precursory to *fracture mechanics*. The methods are computationally demanding, and for the future there is no foreseeable rapid increase in computational possibilities, the relatively slow increase following Moore's law is what we have to live with. Important is also the experimental verification/falsification of the 'predictions' from numerical material science models. Experiments trying to falsify/verify the effect of particle density alluded to in Fig. 3, are rather problematic. In Lilliu et al. (2002) an attempt was made to analyze the effects in uniaxial tensile tests using a new test-method developed in Van Mier and Shi (2002). When the particle content in concrete is increased, the surface area of all the grains grows rapidly, placing a larger demand on the water needed during mixing. The amount of surface-absorbed water increases rapidly, thereby affecting the 'smearing' capability of the cement matrix in the fluid (plastic) phase when the material is produced. As a consequence, an identical matrix quality and ITZ quality cannot be guaranteed for mixtures containing different quantities of aggregates, whereas the effect becomes relatively more important when the size of the grains, or their shape changes; see also in the sections to follow.

It seems imperative to perform 3D analyses, at least for concrete. For materials with a 2D material structure, like laminates, basalt or columnar ice, a 2D analysis may (perhaps) suffice. The experience is that a distinct pre-peak behaviour is observed in 2D and 3D analyses, where a significant inflection point is observed in 3D, which does not appear in 2D. In 2D analyses, like those presented in Fig. 3, cracks always grow through the thickness in one step, whereas in 3D the process is more gradual, and macrocracks are observed to grow through a specimens' cross-section more slowly thereby decreasing the rather large brittleness of 2D-analyses in which a local elastic-brittle fracture law is used for the lattice beams, see Lilliu and Van Mier (2003). On the basis of recent 3D results my opinion has changed, and the most important and interesting stage in the fracturing of materials is regime of (stable) microcracking that is associated with the pre-peak part of the load–displacement curve. The post-peak part of the curve, which has played an important role in research of fracture of concrete materials and structures in the past three decades, seems to be of less interest since the material is actually failed then. Moreover, because structural effects during softening influence the result, softening diagrams measured in a specific structural context cannot very easily be transferred to other structural situations. The pre-peak cracking is inherently stable, determines the strength of a material specimen, and with that scaling of strength, and for that reason is the most important regime where the response of materials can be readily improved, without reverting to draconic measures like the addition of large fibres and/or pre-stressing to arrest the growth of macrocracks. Most optimal is, however, the development of materials where both the strength and ductility are improved, which is for example the case in hybrid-fibre concrete, see Markovic et al. (2003a). In the following section, scaling of fracture strength will be discussed.

4 Scaling of strength

As mentioned in the previous section scaling of strength is important, not in the last place, because —at least for materials like concrete— the material can not always be tested at the scale of the application. Pre-peak microcracking, which is per definition a process stabilized through the presence of material structural elements that are capable of arresting microcracks, is one of the significant factors influencing the strength of materials. Since material specimens tested in the lab are considered small-scale structural tests, there are again two factors affecting the strength of the specimen, namely (i) structural factors and (ii) material-related factors. In many cases the contributions from these effects are mixed-up, and a clear separation is difficult, if not impossible. Some examples will be given after a brief interlude on shrinkage-induced cracking, which is helpful in the discussion to follow.

It is quite well known that shrinkage occurs in cement, and is caused by different reasons such as drying, carbonation, chemical reactions during hydration, and others. The cement phase is the shrinking component in concrete. Aggregates are usually made of non-shrinking material, and depending on their mechanical properties like bulk modulus K, restrain the shrinkage of the cement. This type of restraint can be considered a material effect, see Fig. 5c. Shrinkage goes more rapidly at places where the precise conditions are met. For example in the case of drying shrinkage, moisture loss occurs through the surface where the structure is in contact with a low RH atmosphere. The result is differential drying, where the moisture content of the structure is higher in the core, and lower along the surface. This can be considered as a structural effect since the geometry of the structure (i.e., the exposed area) clearly plays an important role in the drying process for small and large structures. We will return to this point further on. The consequence of differential drying are strain- and stress-gradients, and finally (micro-) cracking as shown in Fig. 5a. The afore-mentioned aggregates can affect the microcracking to some extent, as was shown in extensive experiments by Bisschop (2002). Some of his results are reprinted in Fig. 6, which show that in small prisms of $40 \times 40 \times 160\,\text{mm}^3$, subjected to uniaxial drying along one of the large surfaces, crack growth after 10% moisture loss and 30% moisture loss increases only when the aggregates have a sufficiently large size. The tests of Fig. 6 show that for the larger sized aggregates (4–6 mm) the restraining effect is quite well developed. Consequently microcracking due to aggregate restraint continues during prolonged drying. These results indicate that the shrinkage deformations around the aggregates must be large enough to develop sufficient stress build-up to cause cracks radiating outwards from the surface of the grains, see also Golterman (1995) and Fig. 5c. For small aggregates the total shrinkage deformation is simply too small to cause any radial cracks from aggregate restraint, and the only cracking observed consists of relatively short cracks perpendicular to the specimen surface, see Fig. 5b. This effect is not different from the drying of clay, and on the surface of the structure (in this case the small prism) a network of cracks is formed. Different shaped polygons are recognized, that seems to form cells of different size. The clay cracks often form a clear hierarchical system, where again, when the cell size has reached a certain minimum size, shrinkage deformations are simply getting too small to cause microcracks. Colina and Roux (2000) showed that the size of the polygons depends on the thickness of the shrinking layer as well. The complete analysis of drying shrinkage cracking is quite complicated since one should understand the drying process in the porous material, the shrinkage mechanisms, and the relation between shrinkage strain and moisture content, and all processes must be described in time, see Sadouki and Van Mier (1996), Jankovic et al. (2001), and many others. By means of AE monitoring, Shiotani et al. (2002) demonstrated that the drying shrinkage process in cement-based materials is a very rapid process when no aggregates are included, but as soon as large aggregates are present, aggregate restraint becomes important, and prolonged AE activity is measured. This is in agreement with the results shown in Fig. 6.

Including in a section on scaling a diversion on shrinkage microcracking may look strange. Yet, scaling of strength can be understood when the microcrack processes in the pre-peak regime are understood, and in moisture-prone materials shrinkage leads to microcracks that may even affect the strength of laboratory specimens. In most

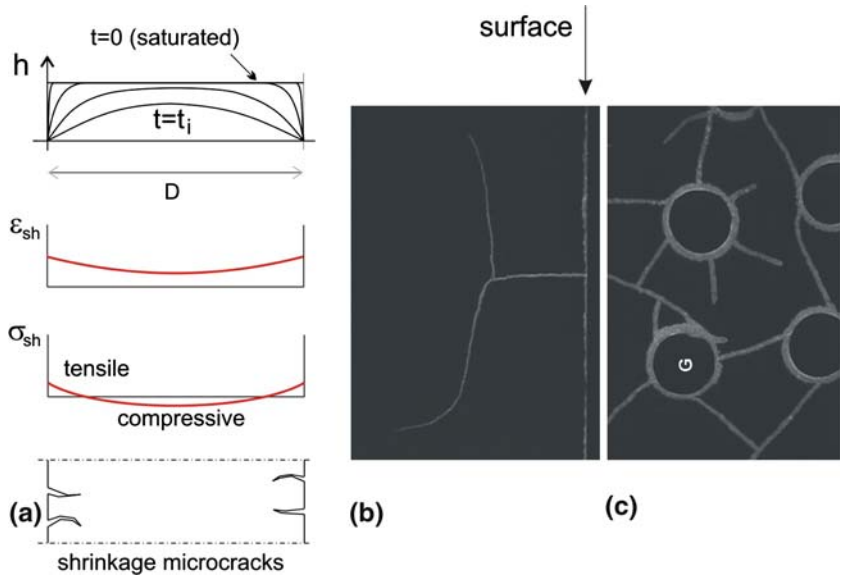

Fig. 5 Shrinkage of concrete: (**a**) structural effect: moisture loss leads to deformation gradients due to shrinkage; since a gradient is present cracking is limited to the surface of the concrete structures (after Van Mier 2004); (**b**) drying shrinkage crack in hardened cement paste perpendicular to the drying surface showing branching; and (**c**) shrinkage cracking due to aggregate restraint, which caused cracks to radiate out from glass spheres that were used as aggregates (after Shiotani et al. 2003)

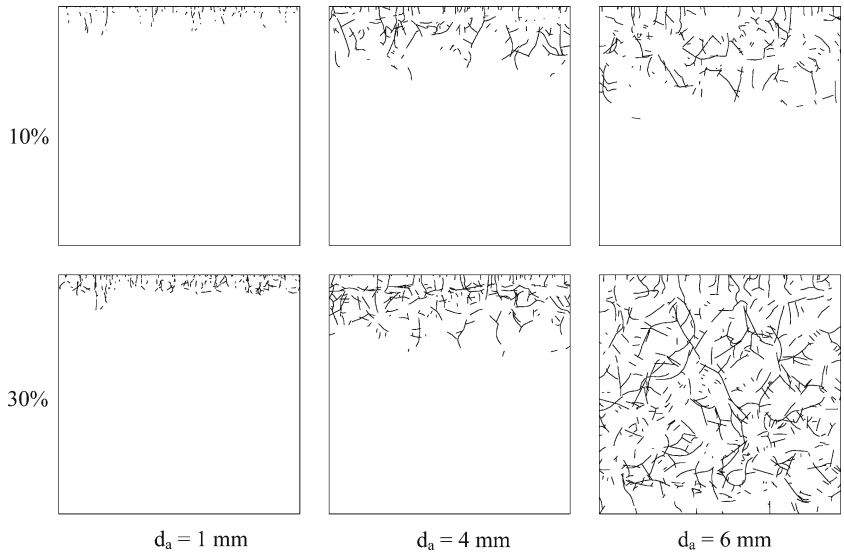

Fig. 6 Effect of aggregate size on drying shrinkage cracking in cement-based materials, after Bisschop (2002). Three cases are shown, for cement paste containing 35% (vol. %) mono-sized glass spheres of diameter $d_a = 1$ mm (**a**) 4 mm (**b**) and 6 mm (**c**) at two stages of moisture loss, viz. 10% of the original water content (top row) and 30% (bottom row). For aggregates smaller than 1 mm no aggregate restraint occurs, and the result is similar to $d_a = 1$ mm

of the scaling laws derived for concrete, e.g., Bažant (1997) and Carpinteri et al. (1995) many different test-results are considered, irrespective of curing and loading conditions and the models can at large be considered as phenomenological engineering models. The size effect law of Bažant is written as follows,

$$\sigma_{\mathrm{N}} = \frac{Bf_{\mathrm{t}}^{'}}{\sqrt{1+\frac{D}{D_0}}}, \tag{2}$$

where σ_{N} is the nominal strength of the structure of size D, and parameters Bf'_{t} and D/D_0 are described by

$$Bf_t' = \sqrt{\frac{G_F E}{kc_f}}; \frac{D}{D_0} = \frac{a_0}{c_f} = \beta. \tag{3}$$

Carpinteri's equation is similarly simple and describes the size-dependent strength with

$$\sigma_N(D) = f_t\sqrt{1+\frac{l_{\mathrm{ch}}}{D}}. \tag{4}$$

Both equations fit rather well to laboratory experiments, in some cases even with correlation

coefficients as large as 0.98–0.99. The difference in the equations lies in the asymptotic behaviour for small and large sizes. Both models contain a parameter that relates to the fracture process, namely, the length of the process zone c_f in Eq. (2) and the characteristic length l_{ch}, which is related to the aggregate size in Eq. (4). Because there are inherent difficulties in measuring process zone sizes, the common procedure is to fit Eqs. (2) and (4) to experimental data sets, and it is easy to see that extrapolation beyond the size limits in the used data sets can be troublesome. It is therefore considered of utmost importance that such engineering size/scale effect models should be completed with a parameter estimate procedure relating the scale factors to physical material parameters. The effect of eigen-stresses due to drying shrinkage does not appear in these models, and differences in curing conditions are hidden in the parameters that give the best fit to a certain data set of tests conducted under certain ambient conditions. When these conditions change, the parameters must be fitted again.

In recent size/scale tests the influence of different curing regimes on the size effect on tensile strength of concrete was explored, see Van Vliet and Van Mier (2000). The results shown in Fig. 7a,b clearly indicate what happens when specimens are kept wet until one day before testing, or when they are allowed to dry very gradually in a laboratory atmosphere, such that no moisture gradients are present in the material at the time of testing. For the case where equilibrium with the environment was obtained, specimens of six different sizes were tested (scale range 1:32); for the specimens with extreme moisture gradients only the four smallest specimen sizes were considered (scale range 1:8). Limitations in transporting the largest two specimen sizes to and from the climate chamber was the reason to reduce the size range in the second test series. In Fig. 7a,b a fit of the measurements with the Weibull model following

$$\sigma_{\mathrm{N}} \propto D^{-n/m} \tag{5}$$

as derived by Bažant and Cedolin (1991) is shown. In Eq. (5) σ_N is the nominal strength, D is the characteristic structure size, n is the number of considered dimensions ($n = 2$ for the tests of Fig. 7, where the thickness is held constant at 100 mm for all specimens) and m is the Weibull modulus, which is considered to be a material parameter. Zech and Wittmann (1978) derived $m = 12$ for a series of tensile tests on concrete.

The Weibull model is a weakest link model, meaning that the complete structure will collapse as soon as the weakest element fails. For this to decide, the structure should be subdivided into N elements of equal size each containing a single defect. Failure of the most critical element would lead to complete rupture. Generally a distinction is made between Weibull scaling and Gumbel scaling (see for example in Alava et al. 2006) where the distinction lies in the distribution of local failure strength. Gumbel scaling would occur when the distribution is relatively narrow; in Weibull scaling a wider distribution is assumed. Materials like concrete have a rather coarse material structure, which results in a rather large Representative Volume Element (RVE). In the tensile fracture scaling tests shown in Fig. 7a,b, the smallest dimension of the smallest specimen was in the neck, and was only 3.8 times larger than the dimension of the largest aggregate included in the mixture (which was 8 mm). For this specimen size a large number of experiments was carried out in order to get an impression of the scatter in test-data. The results of Fig. 7a, b indicate that the scatter for the smallest size was much larger than for all the other sizes. Considering the effects of drying shrinkage, and the constant size of the affected surface layer, one could argue that the RVE for concrete must be chosen as large as 8–10 times d_{max}, which is much larger than the factor 3–5 often found in literature (see Van Mier 2001). Applying continuum theory at small scales is not allowed. Of course one might apply continuum theory in the small scale regime, but should accept that the theoretical result can never be tested against physical experiments. This argument is important, and as a matter of fact, for smaller scales one has to resort to micromechanical analysis, like for example the type of models described in Sect. 3.

The effect of eigen-stresses due to drying shrinkage cannot be ignored. At small scales, below a transition size where the specimen/structure cannot be considered anymore to be a representative volume element, micro-mechanical analysis is essential, and the only way to analyse the strength of the specimen/structure; for large size-scales

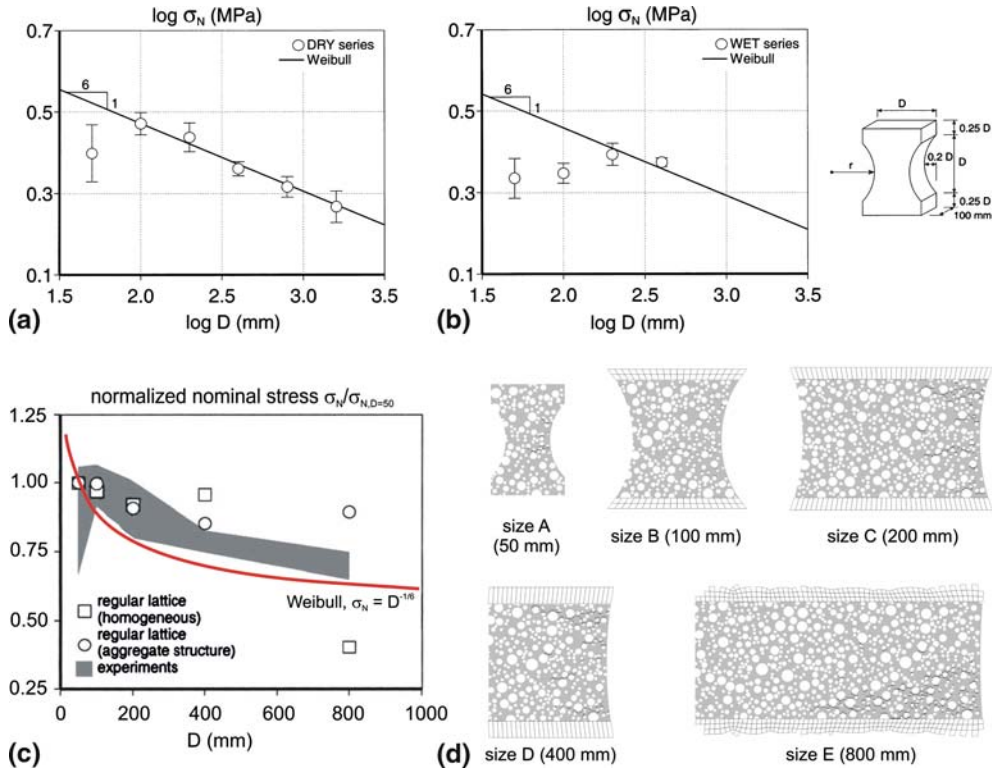

Fig. 7 Effect of specimens size D on tensile strength of concrete ($d_{\max} = 8$ mm) in 2D-scaling experiments on dog-bone shaped plates loaded between freely rotating loading platens for (**a**) specimens where the internal moisture content is in equilibrium with the laboratory atmosphere, and (**b**) where a severe moisture gradient exists due to testing after 1 day drying, after Van Vliet and Van Mier (2000). The experimental data are compared to the outcome of Eq. (5) with $m = 12$ and $n = 2$. Lattice simulations give a size effect, even when the local fracture law is elastic-purely brittle (**c**) but details depend on the heterogeneity in the model. Random lattices have more disorder than regular lattices, which results in considerable differences. The crack patterns at peak stress are plotted for five different specimen sizes in (**d**)

above the transition scale where continuum principles might be applied (although there are other pressing arguments not to do this in the case of fracture problems) Weibull or Gumbel scaling, for example adopting Eq. (5) might be considered but the nominal stress must be amended to include the eigen-stresses due to differential volume changes from shrinkage (or differential temperatures, which results in the same effect). This would lead to

$$\sigma_{\mathrm{N}} + \sigma_{\mathrm{E}} \propto D^{-n/m} \tag{6}$$

where σ_{E} is the magnifying effect from tensile eigen-stresses augmenting the nominal stress from mechanical loading. An alternate approach would be to reduce D to D_{E} but this is more troublesome since the contribution of the micro-cracked surface zones is difficult to estimate. The results by Bisschop reproduced in Fig. 6 give some clue, and actually demonstrate that the material structure cannot be ignored. The tensile scaling experiments of Fig. 7 showed extensive surface cracking, which was attributed to shrinkage (Van Vliet 2000). The shrinkage cracks contribute to pre-critical crack growth in concrete, and directly affect the strength of the material/structure. The notion of material in a structure is important here, since both aspects contribute to scaling; see for example the statistical analyses by Berthelot and Fatmi (2004), who show that significant differences in fracture process under uniaxial tension and flexure exist. In a recent paper, Elkadi and Van Mier (2006) analyzed the

combined material/structural contributions to fracture scaling in hollow cylinders tested under hydrostatic compression (with no stress along the inner hole). In this study it was attempted to separate structural and material related effects in scaling of strength, which is actually the major issue in dealing with scaling laws for concrete (and other quasi-brittle materials like rock and ceramics at various scales, but more about that later). Some important clues were derived from the hollow-cylinder tests. First of all, looking to the stress achieved at different levels of inner-hole deformation (radial deformation) showed that scaling due to stress- and/or strain-gradients in the specimens occurs before the maximum stress is reached. This is clearly a structural contribution to scaling that can not be ignored, and is sometimes referred to as deterministic size effect. Next to that, there was a clear effect of material structure on strength scaling, manifested through a variation of maximum aggregate size in the concretes tested. Quite surprising was that Eq. (2) could be fitted to the test-results by using $n = 3$ for three-dimensional fracture, and the same Weibull modulus $m = 12$, although the correlation coefficient is smaller compared to fits of the Bažant and Carpinteri models. The Weibull fit results in an exponent of $-1/4$ for three-dimensional fracture, compared to $-1/6$ for two-dimensional fracture. Again, this is a rather coarse first-order approximation, and further study should clarify many of the questions that remain. Interesting to note is that in 2D-scaling when the specimen thickness is kept constant, a transition must occur from plane strain to plane stress. This means that for a very small specimen with relatively large thickness plane strain prevails, and for a very large specimen plane stress. This would imply a gradual change of the scaling exponent from $-1/4$ to $-1/6$. When results from 2D-scaling experiments are analyzed using the Weibull theory this change-over cannot be ignored, but, as in all approaches to fracture scaling this argument has always been avoided.

Below the RVE, fracture scaling can only be analyzed by means of micromechanics, for example by applying the type of models presented in Sect. 3. The application of micromechanics models for predicting scaling properties of heterogeneous materials like concrete dates back to the 1980s, see for example Bažant et al. (1990), Riera Rocha (1991), and Elkadi et al. (2006) as well as quite some research done using lattice-type fracture models, see for example Duxbury et al. (1995), Van Mier and Van Vliet (2003), etc. The analyses are rather cumbersome, and take long time, especially for very large structures. The material structure is kept constant, and because the number of elements tends to expand beyond reasonable limits, most scaling analyses are done in 2-dimensions. Full three-dimensional scaling is generally not analyzed, and the results from simulations can be compared to plane-stress situations only.

The dog-bones tested by Van Vliet and Van Mier (2000) were analyzed by means of a beam lattice (see Sect. 3). Only the five smallest specimens were analyzed in view of the considerable computational effort needed. Figure 7c shows a comparison between the results of numerical analyses using both random and regular lattice, the Weibull model with an exponent $-1/6$, and a comparison of the dry scaling tests (see also Fig. 7a). In Fig. 7d five computed crack patterns for specimens sizes (A) through (E) with a scale range of 1:16 are shown. Note that for the two largest sizes only half of the specimen is shown. The crack patterns all correspond to the peak stress level. Since loading was applied with a small (scaled) eccentricity, the cracks always start at the right side of the specimens. The simulated situation matches the experimental conditions exactly. The aggregate content in the analyses was just over 20% (after lattice overlay) which places this result below the percolation threshold of the ITZ. As a consequence considerable pre-peak micro-cracking occurs, as can be seen from the crack patterns.

The Weibull model would apply if immediately upon cracking of the first element in the material structure catastrophic failure would occur. Clearly, the material micro-structure has the capability to re-distribute stresses and to arrest microcracks to some extent, which certainly makes the case for Weibull scaling (and Gumbel scaling) rather weak. The results of the lattice analyses are influenced by the heterogeneity included in the model, and this is larger for the random lattice than for the regular lattice. The randomness of the lattice structure gives an additional heterogeneity, and basically prevents that straight cracks can develop, see Vervuurt (1997). The deviation of the lattice

analyses from the Weibull curve can therefore only be expected. In the experiments, a high aggregate content is used, much higher than included in the model: the density would, as a matter of fact, exceed the percolation threshold for the ITZ found in the analyses of Fig. 3. The comparison between the Weibull model and the experiments seems therefore allowed, yet, as far as the lattice analyses are concerned, they clearly have reached the current limitations of computation. The interesting points are however, that (1) a lattice model based on an elastic-purely brittle local constitutive equation can lead to scaling of fracture strength, and (2) the material composition has an apparent effect on strength, and thus also on fracture scaling. Macroscopic scaling laws like those developed by Bažant (1984) and Carpinteri and Chiaia (1995) give much better fits than shown here, but one has to consider a number of error sources (like the effect of differential shrinkage and the transition from plane-strain to plane-stress in two-dimensional scaling experiments) that were not, or just partly known at the time these models were developed. The multi-fractal scaling law is interesting since it attempts to explain scaling from considerations of the fractal nature of the material structure and the ensuing crack patterns, see Carpinteri (2003). In the approach by Carpinteri and co-workers it is assumed that part of the crack follows the weak interfaces between aggregates and matrix, and that part of the crack traverses the matrix. The results shown in Fig. 3 clearly indicate that there is more to it, and actually the aggregate content has a significant influence where cracks may, or may not develop. Clearly there is room for further research in this area.[1] For the high aggregate contents used in concrete in practice, one has certainly exceeded the percolation threshold, which implies that only bond cracks may develop. Considering a larger range of particles in the multi-fractal scaling law may be important, although one might wonder if the concept of an ITZ of uniform thickness encapsulating all aggregates irrespective of their size is certainly open to further investigation as well. Looking to the meso-level structure in Fig. 1b, one may even wonder if the ITZ concept as used in the lattice model, and many related meso-level models, is correct.

Better models for describing scaling of fracture strength are important since they would allow engineers to determine on small samples how large the expected strength would be in real size structures. For a scaling law to be correct, the physical aspects of fracture must be considered. Missing one single physical effect might make a phenomenological size/scaling law useless immediately, irrespective of the claimed accuracy. The present results show that there is need of better insight on the effect of material structure on fracture scaling. The continued improvement of micromechanics models and the development of better test methods is crucial in this respect. The micromechanics are needed to determine the transition scale from which continuum theories might possibly be applied.

5 What happens at micro-scales and beyond?

Micromechanics models like lattice (Sect. 3), Particle Flow Code (PFC, developed by Cundall and Strack 1979 and applied by Vonk 1992; Iwashita and Oda 2000; Thortnton and Antony 2000; Potyondy and Cundall 2004; Elkadi et al. 2006 and many others) requires certain material parameters like the interaction forces between particles (grains), and/or the strength of cement. It is therefore interesting to investigate what happens in materials like cement (and clay) at very small scales, i.e., at the micrometer scale and beyond. In these materials, water plays a rather important role in defining the level of the cohesive forces between adjacent particles. Other physical mechanisms are active as well, and it depends on the scale of observation which mechanism is active, which one is dominant, and how the actual strength of these materials would have to be interpreted. It is also interesting to ask how the mechanical behaviour of cement scales with specimen (or structure) size, for example when very small specimens are scaled with respect to the grain size of the originally un-hydrated cement grains. As hydration proceeds, the grain size changes, and a new structure built from Calcium Silicate Hydrates (CSH), Calcium Hydroxide

[1] One of the reviewers pointed out a recent paper by Alava et al. (2006) which contains an extensive overview and results from attempts to model fracture scaling by means of statistical models of fracture.

(CH), water, and some by-products emerges. In case of clay the situation is different, and the only forces to be considered are attractive and repulsive forces in water filled capillaries between the small clay grains, electric repulsion and Van der Waals/London attraction forces at very small distances. Chemical bonds are often considered non-existent in clay. For cement the debate is on-going, see for example in Gmira et al. (2004).

The structure of cement is not static, but develops in time, depending on the availability of reactants (un-hydrated cement and water). Several computer models have been developed in past years that are capable, at least to some extent, to simulate the development of the cement microstructure in time. These are quite laborious attempts to come to a description of the material structure-properties relation. Basically, Portland cement, the most common form, contains four different clinkers that react with water. In cement nomenclature,[2] these phases are C_3A, C_3S, C_2S and C_4AF. The reaction with water is called hydration and proceeds only controlled when gypsum is included. The emerging structure is rather complicated, and for a good overview of the matter, the reader is referred to the various publications dealing with cement hydration, for example Bentz et al. (1994) and Bentz (1997) and more recently Pignat et al. (2005). The hydration starts at places where cement comes into contact with water, and results in a complicated microstructure, like the one visible in Fig. 1b (micro-level). As mentioned, the emerging reaction products are CSH and CH, whereas water remains present in micro pore-space formed by the hydrates. Strength is attributed to the CSH, whereas the CH can easily dissolute and contributes very little to strength. The way hydrating cement particles bond together will therefore determine the strength of cement, and is the primary information needed. The afore-mentioned hydration models all have certain elements of the complete process included, but none is perfect, which is no surprise in view of the complexities at hand.

The model developed at NIST by Bentz et al. (1994), Bentz (1997) is a cellular automaton which includes direct geometrical and chemical information obtained on un-hydrated cement grains. All clinkers are included in this model, which is in strong contrast to many of the other models that consider just the C_3S clinker only (e.g., Berlage 1987, which is the original HYDRASIM model on which further developments by Van Beugel 1991; Koenders 1997; Ye 2003 are based under the name HYMOSTUC; Pignat et al. 2005; Maekawa et al. 1999, and others). This limitation might be in order when strength is considered, but when it comes to, for example, simulating pore-space and (saturated/partially saturated) transport properties of fluids accurately, results from models based on spherical cement grains comprising of a single clinker phase should be used with some reservation.

Rather than trying to describe the structure development in minute detail, which would require descending all the way down to the nano-level, it is interesting to limit the effort and try measuring strength and fracture behaviour of cement at the micro-scale. For this purpose various methods can be used, such as micro-indentation (Constantinides and Ulm 2004; Trtik et al. 2005a) or other micro-mechanical tests like flexural or tensile tests scaled down to the level of the individual cement grains. Indentation may lead to rather excessive damage and plastic deformation around the indent (see Fig. 8 and Trtik et al. 2005a), while at the same time three-dimensional artifacts might influence the result. For example, sub-surface pores, or hard regions just below the indenter site are likely to affect the outcome of an experiment, and in general a large scatter in test results is obtained when micro- (or even nano-) indentation tests are done on highly disordered materials like Portland cement, e.g., Schärer (2005). In the latter tests the values for the local Young's moduli ranged between 9 GPa and 53 GPa, indicating in part the variation in materials, but also variation in geometrical artifacts, and non-smoothness of contact surfaces as discussed before. Carpinteri et al. (2004) analyzed the damage done under sharp indenters, and found different types of damage, namely next to chip formation the growth of a splitting crack directly under the indenter's tip, which was recently observed in experiments, see Trtik et al. (2005a).

In order to obtain more information on fracture the development and application of specially

[2] In cement chemistry, abbreviated nomenclature is used: C stands for CaO, S for SiO_2, H for H_2O and A for Al_2O_3.

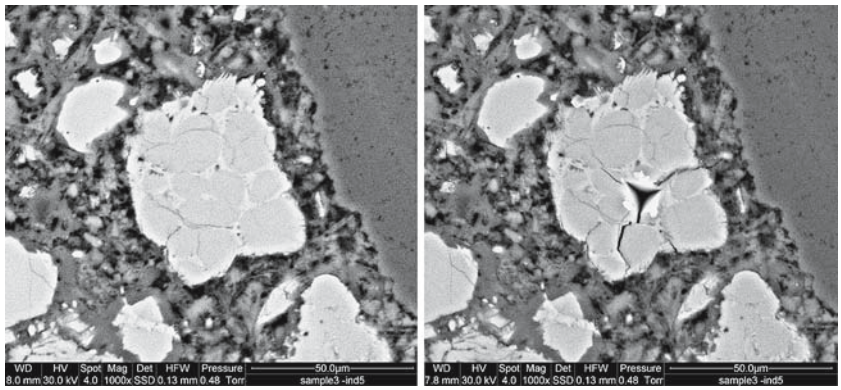

Fig. 8 Indentation with a Berkovich diamond tip in cement paste: indented region before (**a**) and after the indentation (**b**). Note the severe radial cracking emanating from the corners of the indent. In these images, white is the un-hydrated material, different grey shaded are the hydrates, and black is porosity. Note the distinct structure inside the un-hydrated cement grain (various clinkers can be distinguished) that seems to affect crack growth from the indenter edges

designed micro-tensile or micro-flexural tests seems more promising, as was recently pioneered by Trtik et al. (2005b). Disadvantages are the longer development time and the complexity of the experiment (especially in the case of tensile testing) and difficulties in performing the tests owing to its extreme small size. However, the obvious advantage is that the results are easier to interpret because the specimen is not subjected to extreme local stress concentrations. Although only limited data was obtained in a test session at the Swiss Light Source (Paul Scherrer Institute, Villigen, Switzerland), which was used to extract three-dimensional information on crack propagation during the micro-tensile test, the new insight obtained is considered quite valuable, and is essential for the discussion to follow.

From Fig. 1b (micro-level) one could conclude that un-hydrated cement grains may possibly act like rigid aggregates, similar to the function of stiff and strong sand and gravel particles at the meso-level (see Fig. 1b (meso) and the analyses shown in Fig. 3, which clearly show crack deflection by the larger aggregates). The result in Fig. 9 shows the upper and lower crack surface of the main crack that developed in a notched cylinder of size $h \times d = 250 \times 130\,\mu$m. The crack appears to cut through different parts of the material, like the interface between hydrated- and un-hydrated cement, straight through the hydrates, but also through the un-hydrated particles, which shows that they cannot un-restrictedly be regarded as hard, tough obstacles deflecting the path of the crack, as is common for gravel particles at the meso-level. The experiments also revealed very small crack face bridges, of sub-micrometre size, connecting the two crack faces in advanced stages of crack growth (see the small white patches in Fig. 9, after Trtik et al. 2005b). A few years earlier, small scale bridging (μm-scale) was observed in the cement-microstructure under drying conditions leading to shrinkage cracking by Bisschop (2002). At the meso-level, bridging was found to be directly related to the long tail in the softening diagram (as was first discovered by Van Mier 1991a,b) and the present result would suggest that softening happens at the micro-scale in hardened Portland cement as well. Note that in the simple models presented in Sect. 3 the assumption was made that fracture in all three material phases distinguished at the meso-level (i.e., cement matrix, ITZ and aggregate) behave following a simple elasto-purely brittle fracture law. Strength loss is immediate after a certain threshold is exceeded. The new results from the micro-mechanical experiments suggest, however, that one can also expect different type of behaviour, viz. crack bridging of the main crack leading to the long tail of the softening diagram. Most likely the details of the hydrated cement structure may prove to be important in the

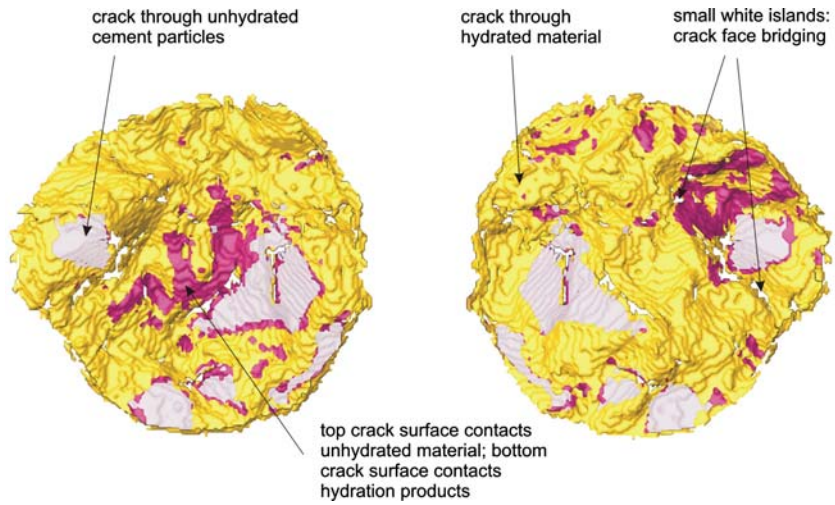

Fig. 9 Crack bridging in pure cement paste at the micro-scale. Bridges appear as white spots in this image of an internal crack surface in partly hydrated Portland cement at the micro-scale, after Trtik et al (2005b). Cracks appear to grow through hydrates, but also through un-hydrated material and along the interface between these two phases

process, but for that purpose more extensive testing is needed.

It is interesting to pursue this line of reasoning a bit further. In concrete, cement paste patches may have extremely small dimensions, especially at places where two aggregate particles approach one another very closely. Breaking of such 'cement-ribbons' is a quasi-brittle process, which may explain why the simple elasto-purely brittle lattice model under-estimates the post-peak ductility like in the analyses of Fig. 3. Thus, the result of Fig. 9 suggests that softening may occur in small samples just a few cement grain diameters across (the typical size of cement grains is between 10 μm and 100 μm). Moreover, softening was first observed in concrete and rocks, which must be attributed to the relatively large heterogeneity of these materials: in macroscopic samples of concrete typically about 6–7 maximum grain sizes can be placed across the smallest dimension (16–32 mm aggregates in a 100–150 mm specimen), which leads to a similar D/d_a ratio as in the afore-mentioned micro-tensile test; see Sect. 4. Note that after full hydration the microstructure of cement has changed and the above remark on heterogeneity of hardened cement past should be amended.

Several factors must be considered in the hydration process, namely, the size of the cement grains (which defines the cement area exposed to water) the clinkers that make up the cement grains, the possible internal structure of the cement grains (which is clearly present, see for example in Fig. 8a) the amount of water available for the hydration process, whereas temperature plays an important role in the process as well.[3] Depending on the time elapsed after mixing the various constituents, hydration has proceeded to some extent into the cement grains. The process as a whole is very complicated (as may be evident from the large amount of literature in the field), the difficulties encountered in testing at extreme small size scales, and the moisture sensitivity of the material structure, see for example Jennings (2000) and Tennis and Jennings (2000). In general two types of CSH are considered, referred to as "low-density (LD-) CSH and high-density (HD-) CSH", or "outer-product and inner-product", or "early- and late-CSH" (Jennings 2000; Taplin 1959; Constantinides and Ulm 2004). In the latter paper it was suggested that significant differences in elastic properties (stiffness) can be observed by means of nano-indentation, but recent attempts to confirm these results have not been very successful to date (Schärer 2005). What certainly happens during hydration is that the size of the hydrated shells around the un-hydrated kernels will gradually increase, and the total volume taken by CSH will rapidly exceed the volume of un-hydrated material. This has been

[3] Temperature rise in hardening cement at early ages may cause similar problems as differential drying discussed in Section 4 (see Fig. 5). It is no problem that temperatures may rise up to 60–70 °C during hydration, but as soon as temperature gradients develop due to subsequent cooling, microcracking may occur and cause serious problems.

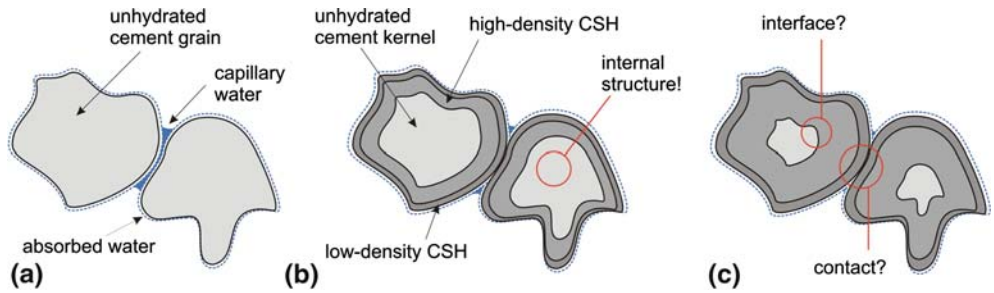

Fig. 10 Schematic hydration process between two cement grains, showing the gradually diminishing un-hydrated kernels and the slowly increasing LD- and HD-CSH shells around those kernels. Time increases from images (**a**) to (**b**) to (**c**). Note the encircled areas in (**b**) and (**c**). Un-hydrated cement has a clear structure at the same scale as the cement particles themselves, and according to the fracture tests of Fig. 9 this cannot be ignored. Big question remains the nature of interfaces between un-hydrated and hydrated HD-CSH, and between adjacent hydrated cement grains (see **c**)

shown schematically in Fig. 10. The strength of the hardened cement paste will depend on the strength distribution in the constituting phases, which are the low- and high density CSH, the un-hydrated cement, and the interfaces between the hydrated cement grains and the un-hydrated and hydrated phases. Compared to the material structure at the meso-scale, the micro-level model would include two types of CSH, un-hydrated cement, and two types of interfaces. Including a possible structure inside the un-hydrated cement grains makes the analyses even less accessible. At any time during the hydration process, depending on the often used 'degree-of-hydration' parameter α, the shell of LD- and HD-CSH will have varying thickness. The relative differences in strength and stiffness between these phases will determine the mechanical response of the cement at a certain age, where, as in any fracture problem, the size of the sample, and the size of the grains in the sample will play a significant role as well. As far as that goes, all the issues mentioned for fracture at macro- and meso-levels in the first part of this paper apply to fracture of cement at the micro-scale too. The micro-model is shown schematically in Fig. 11. The serial spring depicted in this figure shows the main interactions only: un-hydrated cement, LD- and HD-CSH, and the respective interfaces between these phases. When a lattice overlay would be used, as shown in Fig. 2c for concrete at the meso-level, the complexity increases due to the increasing number of material phases that must be considered, and of course the different types of interfaces.

In the example of Fig. 9, the crack crosses through the un-hydrated cement kernels, which were still quite large owing to the relatively young age of the samples at the time of testing. It is hypothesized that the balance may swing in another direction when the hydration shell of LD- and HD-CSH becomes thicker. Future testing would have to show more detail of the fracture process in cement at various degrees of hydration.

6 The role of water at the micro-scale

Particle size and water play some role in defining strength of cement and clay, simply by providing capillary attraction between adjacent particles. Although simplified—electrostatic forces and other interactions are neglected for the moment—there may be some insight in how the strength is built up by looking simply to particle stacks. Using monosized spheres as particles, two different types of packing are considered: the regular packing, where a box is filled by placing the spheres directly on top of each other, and the densest regular packing for spheres, the hexagonal close-packing. Both variants are shown in Fig. 12.

Consider now boxes as drawn in Fig. 12, and fill them with spheres as indicated. The box with the regular stack contains fewer spheres than the box with the hexagonal close-packing (hcp), especially when partial spheres are allowed, i.e., when in the case of hcp the box walls intersect with the particles (see Fig. 12b). The densities of the two types of

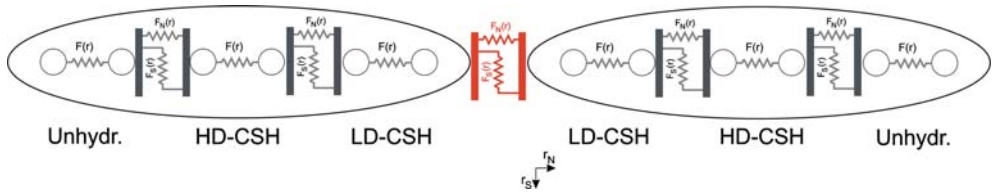

Fig. 11 Main factors in a micromechanical model for cement shown as interaction between two partially hydrated cement grains. In the grains, several phases are recognized, namely un-hydrated, cement and low- and high density CSH (LD-CSH and HD-CSH). Between all phases interface elements must be included, whereas the interaction between the two cement grains is schematized as an additional interface element. In order to include temporal effects, dash-pots can be included

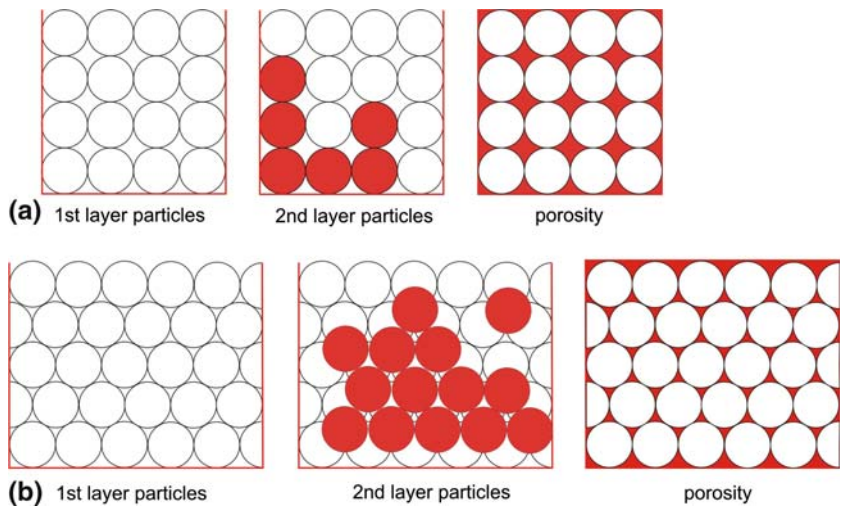

Fig. 12 Regular packing of mono-sized spheres (**a**) and hexagonal close-packing (**b**)

packing, regular (rp) and hexagonal close packing differ markedly. As one would suspect the regular stack contains far less spheres in the same volume, and thus

$$\varphi_{\mathrm{rp}} = 0.5236 \ll 0.7405 = \varphi_{\mathrm{hcp}}. \tag{7}$$

The specific surface scales with the number and size of the spheres. If one decides to keep the size of the box constant, and decrease the size of each sphere by a factor 10, the number of spheres in a box increases by a factor 1,000. The total sphere volume remains constant, but the total area of all spheres increases by a factor 10.

Typical interactions between particles of small and large size depend on the size of the particles. One can distinguish, at very small scales, hydrogen bonds, primary chemical bonds, double layer forces and Van der Waals/London attraction. At somewhat larger scale the capillary forces caused by water layers in the material play a role. These attraction forces depend on the particle size and the amount of water present. The sum of all these interactions is a potential that describes the force–distance relation between two neighbouring particles. Depending on the relative importance of these contributions, the potential will take a certain shape, for example as sketched in Fig. 13a. For the sake of the example, it is assumed that only capillary forces make up the potential. Decreasing the particle size, while maintaining the total water volume in the porous packing of spheres constant, will lead to an effective decrease of the water layers attached to the spheres. The radii of all menisci will decrease, and with that the interaction force p_{d}, which is described by the Laplace equation

$$p_{\mathrm{d}} = \frac{-2\gamma}{r}, \tag{8}$$

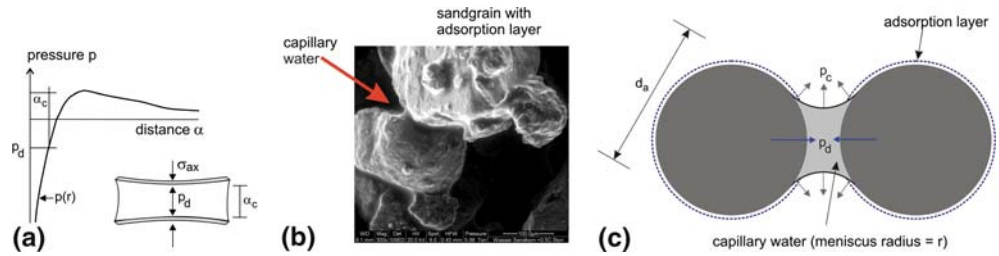

Fig. 13 (**a**) Interaction potential between two (spherical) particles. At the smallest scale this resembles atomic potentials; at larger scales other interaction forces contribute. The challenge is to unravel the contributing factors for interactions between cement particles. Capillary forces caused by water menisci are one of the contributing factors. (**b**) shows an example of a water meniscus between two adjacent sand grains observed in ESEM. The attraction forces between neighbouring particles depend on the radius of the particles, the amount of water, and the relative vapour pressure, which all affect the menisci radii (**c**)

will increase (see Fig. 13c). In Eq. (8) γ is the surface energy for the air-water interface. Thus, under decreasing water content the material (that is, if it can be regarded as such), will become stronger. In three-dimensions the water 'bridge' between two adjacent particles must be considered, and contributions to the tensile strength of the water layer between two spherical particles has two contributions, one from the internal pressure, and a second from the surface tension along the water–air contact:

$$F = \pi r_0^2 p_\mathrm{d} + 2\pi r_0 \gamma \tag{9}$$

where p_d is given by Eq. (8) with $r = r_0 + r_1$, which are the radius of the smallest cross-section of the water column between the two particles and the radius of the meniscus respectively. Now, this is nothing new, for example the mechanism was included in a discrete element model by Muguruma et al. (2000), but the import point to consider is that the geometry of the material plays an important role in deciding its strength.

Of course the example is valid only when all particles have the same size, when all water layers are of identical thickness and when the menisci radii are equal as well. In the heterogeneous material structure of cement and concrete (and clay) the distribution of water is not homogeneous. Water will fill small pores first, whereas at a given relative humidity large pores will only be saturated partially. Therefore, the equilibrium is quite easily disturbed, which can for example clearly be seen in the case of drying shrinkage. When water evaporates from a system where particles do not have equal size, and thus the pore-size distribution is not homogeneous either, the water absorption at the pore walls must be considered in relation to the water vapour pressure in the pores. According to the Kelvin equation,

$$\ln\left(\frac{p}{p_0}\right) = -\left(\frac{2\gamma V_\mathrm{m}}{RT}\right)\cdot\frac{1}{r} \tag{10}$$

where p/p_0 is the relative vapour pressure, γ is the specific surface energy (= 0.072 J/m^2 for water), V_m is the molar volume of the fluid (18.10^{-6} m^3/mol), and r is the pore radius, the relative vapour pressure increases with decreasing pore radius, forcing small pores to fill up already at relatively low external relative humidity. Thus, the above argument of decreasing radius of the water menisci might be nullified due to water vapour exchange with the environment. In a disordered material, coming back to the argument to be made, the places where small particles meet create smaller pores, and thus these might fill up with water quite easily. It will be obvious that at some places in the material the attraction is larger than at other spots, consequently leading to relative movement of particles with respect to each other. These movements are constantly updated as the water moves in the particle system, but ultimately, attractive regions will develop, and the result is obviously the creation of 'canyons' devoid of water when the distance increases and the attractive role of

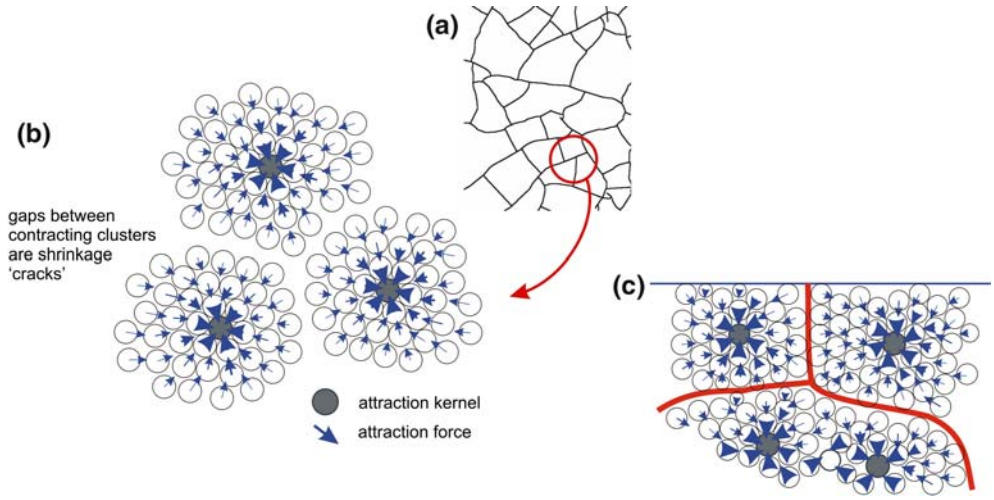

Fig. 14 Relative motion of small particles bonded by capillary forces only in a disordered material will ultimately lead to shrinkage 'crack' patterns like those depicted here. The attraction starts from kernels where bonding through water films is strongest (depicted by larger arrows) and causes larger particle distances and lower water bridging forces at locations farther away from the attraction kernel. At sufficiently large particle separation the water bridge breaks causing a large gap that is interpreted as a 'shrinkage crack'. (**a**) shows a shrinkage crack pattern observed in plain hardened Portland cement with typical cell size of 55–90 mm. The cluster formation in (**b**) is a schematized view of the drying top surface. (**c**) shows a vertical cut, where often horizontal crack branches are observed in experiments. Additional drying through the cracks and capillary suction are believed to contribute significantly to this 'crack'-branching. Note that moisture escapes through the top-surface in (**c**); deeper inside the structure the water content is more uniformly distributed, and the water-particle system will be in equilibrium. As a consequence deep inside the structure movement of particles towards certain attraction kernels will not occur

water diminishes. Capillary suction may eventually play a role as well (Wittmann 1978). The formation of shrinkage 'cracks' arranged in regular cells, as sketched in Fig. 14 is ultimately caused by the above mentioned mechanism. The role of shrinkage is important in cement-based systems: see for example the effect on fracture strength scaling in tension discussed in Sect. 4 (see Fig. 7). In statistical physics several models were proposed for describing shrinkage cracking, see for example Meakin (1991) and Leung and Néda (2000). In such models mostly spring-block systems are analyzed, and no relation exists with the amount of water in the material. A more realistic model should, however, contain this coupling: a moisture flow analysis is needed to estimate the size of water 'bridges' between adjacent particles, and thus the magnitude of the particle binding forces.

Note that small grains lead to more contacts (scaling of the number of contacts is the same as scaling the number of particles in a fixed volume, thus when the number of particles increase by a factor 10^3 due to a size decrease by a factor 10, the number of contacts increases by a factor 10^3 as well), but this not necessarily means that the material will become stronger. The dynamic equilibrium with the environmental humidity must be considered. Note that when the shape of the particles changes, for example, take the shape of M&M candies, the number of contacts increases substantially (Donev et al. 2004), but again, one has to investigate what happens to the water phase. Simulations including realistic grain sizes and grain contacts, like in the NIST Model (Bentz et al. 1994), are considered essential to derive valid behavioural laws.

Cement-based materials have an incredible complicated pore-structure, and only recently attempts have been undertaken to map the microstructure using advanced tomography equipment, for example the Swiss Light Source near Villigen (e.g., Stampanoni 2002), and other facilities, see for example Bentz (2000), Pignat et al. (2005) and Trtik et al. (2005a, b). The problem in these

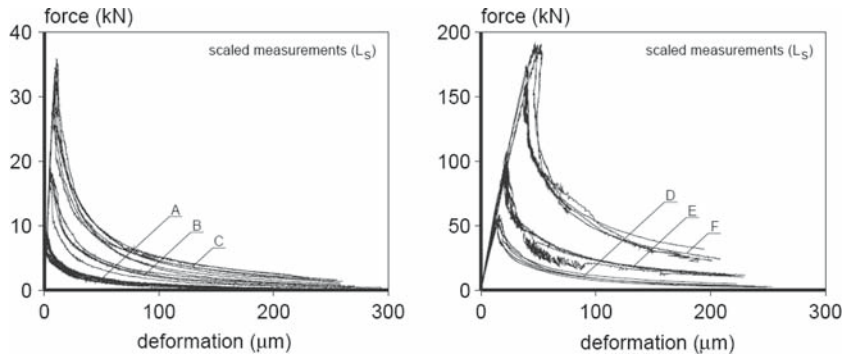

Fig. 15 Force-deformation diagrams from uniaxial tension tests between freely rotating loading platens on dog-bone shaped specimens of varying size in a scale range of 1:32, after Van Vliet and Van Mier (2000); see also Fig. 7a,b for the definition of the size parameter D. The smallest specimens, type 'A', have a length of 75 mm, which is doubled for each subsequent specimen type, up to 2,400 mm for type 'F'. Note that the force scale in (**a**) differs by a factor 5 from that in (**b**)

measurements is that the resolution is not sufficient and pores smaller than 1 μm are missed, which is exactly where matters become highly interesting. Tomography methods are preferred above conventional mercury intrusion porosimetry, which potentially damages the material too much; see also Diamond (2000). A known deficiency of mercury intrusion porosimetry is the 'ink bottle effect', which leads to overestimating the volume taken by the smallest pores. Conventional SEM where samples are observed in vacuum has a number of similar objections, but ESEM is an improvement already (Ye 2003), although of course only two-dimensional information is obtained in that way. Tomography using Focused Ion Beam milling has high accuracy, but is very time-consuming, and samples are machined in vacuum as well, see for example Holzer et al. (2004). The measurements do not have the required resolution yet, but improvements in tomography techniques in the coming years might overcome the current problems. On the other hand, the numerical simulations are rather demanding too, and only small volumes of material over short intervals can be analyzed.

In conclusion, the interactions at the micro-scale between cement grains are numerous, and the relative importance of the various forces, plus the relative stiffness differences, combined with the complex role of water, will define what the strength of the material will be. We are at the brink of a new and exciting research area, where possibly clues can be found for optimizing the grain structure in order to achieve the highest possible strength of cement, if possible in combination with the highest feasible ductility. Regarding model development, the question must be posed how a possible model could look like, considering the current limitations in computation and experimentation. This will be the topic of the next section.

7 Micromechanics at different size/scale levels or stacked continua

Stress-deformation diagrams obtained on specimens of varying size subjected to uniaxial tension show distinct softening behaviour. Not only the tensile strength varies with size/scale, but also there are marked differences in the post-peak diagram. Carpinteri and Ferro (1994) measured the tensile stress-deformation behaviour for a size range of 1:8, and more recently Van Vliet and Van Mier (2000) obtained stable diagrams for a size range of 1:32. The diagrams look different depending on the deformation that is plotted along the x-axis. If the measurement length is scaled with the specimen size, the diagrams of Fig. 15 are obtained. For clarity results have been plotted in two diagrams: one showing the three smallest sizes, the other the three largest sizes. The gradual decreasing slope of the softening diagram is perhaps the most significant difference: for the largest sizes snap-back

behaviour was observed, at least in this representation. It is important to understand that the tests were kept stable by means of an active control, in which the regulation of the servo-valve was done on basis of the displacement transducer that showed the largest absolute deformation. The switching between the various displacement transducers was fast enough to achieve stable softening response.

7.1 Brittleness

Ignoring for the moment all kinds of structural effects that affect the shape of the softening curve, the diagrams could be interpreted as follows. The elastic energy release is increasing with the volume of the specimens, and since the fracture energy increases with the fracture surface only, effectively the balance is disturbed and fracturing will become increasingly un-stable. Brittleness numbers suggested in the past by several researchers, see for example Carpinteri (1985)

$$S_{\mathrm{E}} = \frac{G_f}{f_{\mathrm{t}} h} \tag{11}$$

where $G_f = \int_0^{w_{\mathrm{c}}} \sigma(w)\mathrm{d}w$, the area under the stress-crack opening diagram of the material considered, f_{t} is the maximum tensile strength, and h is the height of the considered structure, attempt to describe the relative brittleness in a simple and straightforward manner. When the value of S_{E} decreases, the behaviour of the structure is extremely brittle and may ultimately show snap-back behaviour, whereas as S_{E} increases, the response changes to more ductile. For the concrete used in the experiments of Fig. 15 the fracture energy and the tensile strength should be the same irrespective of the specimen size, at least, if these parameters can be considered as true material properties. This is clearly not the case, see Van Vliet (2000).

Brittleness and toughness were also discussed by Elfgren (1989), and he suggested writing the brittleness number in the following simple manner:

$$B = \frac{\text{elastic} \cdot \text{energy}}{\text{fracture} \cdot \text{energy}} = \frac{L^3 f_{\mathrm{t}}^2 / E}{L^2 G_f} = \frac{L f_{\mathrm{t}}^2}{E G_f}, \tag{12}$$

which includes the Young's modulus of the material as well. These approaches are interesting in the sense that they try to combine structural and material aspects of fracture, albeit, without consideration of the true fracture process. In Sects. 3 and 4, it was shown that for concrete the rough heterogeneous material structure decides how the material will fracture. It can easily be shown that the fracture energy of two materials may be the same, but their brittleness, interpreted now as the slope of the post-peak softening curve (determined in experiments on specimens of identical size and shape) may be quite different. So, ultimately, there is a need to connect the macroscopic fracture parameters to processes acting at lower levels of observation. For materials like hardened Portland cement, specimens of dimension 100 mm show quite brittle behaviour, and the only way to achieve stable softening is by allowing the crack to arrest itself in a bending moment that develops when loading is applied between non-rotating loading platens, see Van Mier (1991a). Without this precaution it is not possible to achieve stable softening for cement, also not in compression, e.g., Spooner et al. (1976). At smaller scales, fracture in cement might be quasi-brittle, like concrete. Although no stable crack growth was achieved in tensile tests on cement using samples that were a factor 1,000 smaller, i.e., cylinders of diameter 130 μm, the test results showed the appearance of crack face bridges, apparently formed in the same way as observed earlier at large scale in concrete (i.e., compare Figs. 4 and 9). *This would imply that bridging appears in hardened cement paste at a sufficiently small scale, and basically that some form of softening is present at those small scales.* Undoubtedly, all structural constraints and size/scale effects apply at the meso/micrometer scale, similar to those mentioned before. Considering then the small thickness of cement-paste ribbons between aggregates in concrete at the meso-scale, this result would indicate that some softening relation would have to be used in micromechanical analyses of concrete (Fig. 1b (meso) shows how close aggregate particles approach one another, although one should be careful drawing such conclusions on the basis of 2D images like presented in this figure).

The brittleness number proposed by Elfgren (Eq.(12)) is interesting since it includes the size of

the structure. Equation (12) states that large structures behave more brittle than small ones made of the same material. Experiments show that the fracture energy G_f, as well as the tensile strength f_t are size dependent parameters, and as such cannot be designated as true properties of the material. Equation (12) should therefore be re-written as,

$$S_E = \frac{Lf_t^2(L)}{EG_f(L)}, \tag{13}$$

which includes the size dependency of the material properties: both f_t and G_f are functions of size, or alternatively, a reference size must always be defined. For G_f, this may be relatively simple, since its value approaches an asymptote as the size of the structure increases. For the strength f_t the situation appears to be more complicated, although in some size effect models an asymptotic value of the tensile strength for very large sizes is assumed. *The solution might be found in replacing the softening diagram, i.e., stress–displacement (or crack-opening) relation, by a force–displacement relation*, which could possibly better handle the structure (construction) dependency of the softening parameters. For a force–displacement relation, the brittleness number would change to

$$S_E^{alt} = \frac{LF_u^2(L)}{kW_f(L)} \tag{14}$$

where $W_f(L)$ is the size-dependent work of fracture (i.e., the area under the post-peak force–displacement relation at any size scale) and k is the initial stiffness of the spring that represents the fracture potential. More about that is to follow.

In Fig. 15, the stress-deformation diagrams are shown with scaled deformations. This means that the measurement base for each specimen size was chosen proportional to the length of the specimen. As mentioned, for controlling these tests, an advanced electronic system was used, that allowed to switch from one displacement to another, measured on a much shorter measurement base of 75 mm, which was the same for all specimen sizes (Van Mier and Van Vliet 2003). The snap-back behaviour observed for the largest specimen sizes ('type F' in Fig. 15b) does not occur when the deformations are measured over the control measurement length. This is a well-known fact, and reducing the measurement length to the point where it just contains the localized crack, leads to increasingly shallower post-peak behaviour. This again demonstrates that softening is to a large extent a property of the structure, and not only of the material.

7.2 Softening stress-crack opening relation

Reading through the literature on concrete fracture reveals a wealth of proposals for the stress-crack opening relation in tension, ranging from simple linear, bi-linear or multi-linear to curvilinear diagrams, for example a power law. In the meso-level lattice model presented in Sect. 3 of this paper, a special form of a linear softening relation was used, namely the purely brittle mode. As mentioned, Ince et al. (2003) proposed to use a softening relation in meso-level lattice models, but since no measurement results are available at this scale, the choice for a purely brittle law seems more appropriate as argued in Van Mier (2004). An example of a simple softening power law proposed by Foote et al. (1987), based on macroscopic uniaxial tension tests on plain concrete and considering the post-peak behaviour only, is

$$\frac{\sigma(x)}{f_t} = \left[1 - \frac{w(x)}{w_f}\right]^n, \quad n > 0, \tag{15}$$

where n is an exponent that describes the relative ductility of the material, $\sigma(x)/f_t$ the dimensionless softening (or cohesive) stress, and $w(x)$ denotes the crack opening displacement. Note that Eq. (15) considers the material separated from its structural environment. The specimen/structure size affects the softening diagram (see Fig. 15), inclusive the tensile strength f_t. This size effect is not described by Eq (15); a size dependent exponent n would be needed. For large n the material is extremely brittle, for small n, the response becomes plastic. The model, like all the others, is phenomenological in nature, since the parameters n, w_f and f_t are all described independent from the structure of the material. The fracture process, which has been carefully unraveled in the

preceding sections of this paper, is simply considered as a single energy dissipating mechanism, and the only condition for crack nucleation is exceeding the material's tensile strength; and for crack propagation, the fulfillment of the phenomenological softening law, which is basically an energy criterion. In applying these approaches, it is not important whether a microcrack zone propagates in advance of a stress-free crack, or whether wake-bridging leads to the softening response, or even, whether energy dissipation is caused by the growth of a straight crack or an undulating (fractal) crack or a crack involving large frictional energy dissipation.

7.3 Atomic potentials

How should quasi-brittle (or cohesive) fracture models be improved? The answer may be found in a size-dependent description of the softening law augmented with the pre-peak behaviour. The fracture relation can be considered as a potential describing the cohesion between two neighbouring material elements, from the fully intact state to the fully ruptured material. For tension and compression the potential takes a different shape as the underlying physical mechanisms are different. Continuity in the description from the atomic to the macroscopic size/scale exists, in the sense that all diagrams look similar, and comprise of a rising branch from the equilibrium state, a maximum stress (or energy), and subsequently a falling branch or softening branch. This is the case for the atomic potential, but also for softening relations at any size-scale. In spite of that similarity the processes underlying the various diagrams are quite different, or are they? There are at least some marked differences. In general softening diagrams are all (partly) based on continuum ideas of stress and strain (see for example the underlying original experimental results by Evans and Marathe 1968). The new issue of the Hillerborg model was that the notion of strain was dropped in favour of displacement (or crack-opening) as state variable. At the atomic level potentials usually describe the interaction energy or interaction force between two atoms based on their mutual distance r. Famous is the Lennard-Jones potential, which was developed to describe the interaction between atoms in liquefied noble gases,

$$\frac{V_{\mathrm{LJ}}(r)}{\varepsilon} = -4\left[\left(\frac{\sigma}{r}\right)^{12} - \left(\frac{\sigma}{r}\right)^{6}\right] \tag{16}$$

where σ and ε are units of length and energy, respectively.

Bringing the atoms closer together from their equilibrium point at the separation distance r_0 requires a substantial force (or amount of potential energy). Forcing distances smaller than r_0, and provided that the confinement of the system is strong enough, the atoms may either break down into sub-atomic particles, or they may merge to form a new element. The slope of the Lennart-Jones and other potentials is very steep when it comes to bringing atoms close together, indicating the enormous energy required to overcome the repulsive forces. Many interaction potentials can be found in literature, see for example Stillinger and Weber (1985), Bazant and Kaxiras (1996), Bazant et al. (1997), who all provide potentials for Si–Si interactions, including interactions involving more that two atoms, which can be applied in molecular dynamics simulations of the behaviour of solids, e.g., Holland and Marder (1999). The Stillinger–Weber model appears to be quite useful, although, in order to simulate brittle behaviour of a diamond lattice, a coupling term had to be doubled in order to achieve realistic results (Holland and Marder 1999). This signifies that a general applicable potential for silicon is non-existent, and one thus generally finds that semi-empirical potentials are used. In that the problem is not much different from defining softening stress-crack opening relations proposed for modeling cracking at the macro-level. These σ–w diagrams (for example Eq. (15)) are always empirical relations.

7.4 Multi-scale interaction potentials

Thus, the interesting question to ask is whether a continuous potential, ranging from atomic to macroscopic size/scales can be used. The potential function describes at each intermediate scale how a two-particle interaction should be handled. At each size/scale level, there would be different

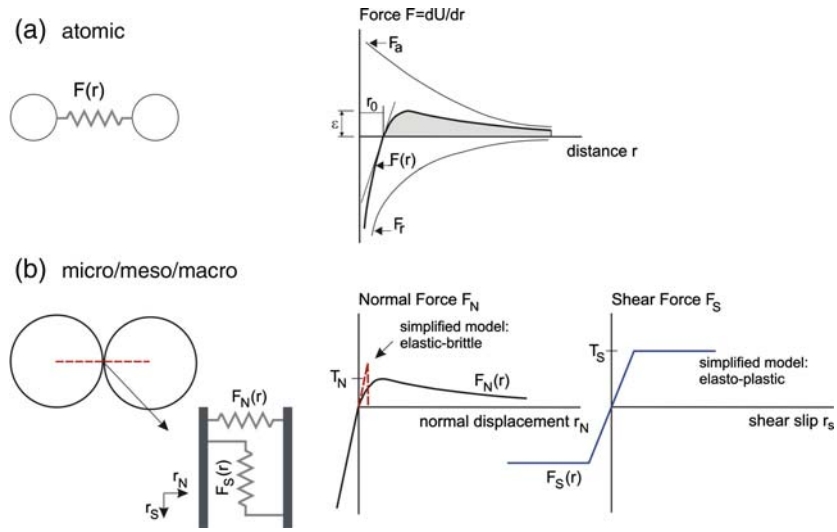

Fig. 16 (**a**) Interaction between two atoms is described by means of a potential for the interaction energy or force (diagram adapted from Visser 1998) and (b) interaction potential for two particles at the micro-/meso- or macro-scale where the particles have physical dimensions ranging from [nm] to [m]. Next to the normal interaction potential, shear interactions must be considered, basically described through a friction coefficient μ

underlying mechanisms leading to the respective potential curve. Multi-scale analysis would have to lead to the right potential at any higher scale. Apparently the size/scale effect might be solved in this way. There are a number of advantages in such an approach, but also some problems, that will be clarified in the following paragraphs.

The model to start with is based on interactions between two spherical particles. Atoms are also considered as spheres, with a spring indicating the interaction force, see Fig. 16a. At an equilibrium distance r_0, the atoms do not interact, and the force is zero. At the atomic scale, the distance at which atoms are 'at rest' is not zero, but has a certain length r_0. At larger size/scales, a distinction is made between 'compressive' and 'tensile' loading, and the equilibrium point is placed in the origin of the stress–displacement space.

A possible force–displacement potential that can be used at different size/scales may be formulated as an extension of Eq. (16):

$$\frac{F}{F_u} = \alpha \left[\left(\frac{\sigma}{r}\right)^m - \left(\frac{\sigma}{r}\right)^n \right] \tag{17}$$

Again σ is a unit of length (which can vary at each size/scale), r is the displacement between the spherical particles (which are atoms at the smallest considered scale). The force F_u is the size-dependent parameter in Eq. (17). Figure 17 shows the potential function F/F_u for $n = 6$ (similar to

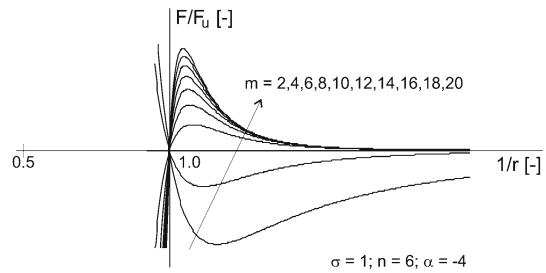

Fig. 17 Interaction potentials in terms of (dimensionless) force F/F_u and separation r. Depending on the model parameters repulsive and attractive regimes may change. The challenge is to determine the physics underlying such forces-separation relationships at any length scale from atomistic to macroscopic

the corresponding exponent in the Lennard-Jones potential) $\alpha = -4$ and $\sigma = 1$. Repulsive and attractive actions are dependent on the value of m with respect to n. When $n = m$, the obvious result $F/F_u = 0$ is obtained. At a certain scale level L, the maximum load $F_u(L)$ has a given value. The function $F/F_u(L)$ takes a certain shape, which is measured in an experiment conducted at the relevant size/scale L. This potential can be used directly in a lattice model (see Sect. 3), but because of its non-linear form would require an iterative solver. The form of the lattice is not very important, except that central force lattices are less suitable for simulating fracture. Instead a beam lattice with a certain angular stiffness would perform better, and also in

that case there is no pressing reason to divert from a normal force potential like, for example, Eq. (17).

It is not the intention here to dwell on the exact form of an interaction potential, but rather to discuss *philosophical implications* of a certain choice. The Lennart-Jones equivalent serves merely as a convenient example that can be used in numerical analyses because it is a continuous function. In contrast, a hard-sphere potential would include a discontinuity leading to numerical problems. Note that the Foote et al. Equation (15) is limited to describing the post-peak curve, and therefore provides a partial representation of the fracture behaviour only. In cohesive models the pre-peak curve is generally simplified to a straight line, defined by the Young's modulus and the tensile strength. Here it is suggested that a continuous function should be used in current cohesive models for describing the complete stress-deformation behaviour at the macro-scale. Then of course, the division in a pre-peak stress–strain and a post-peak stress-crack opening diagram is not possible anymore. The original Hillerborg assumption breaks down, and new approaches must be found.

In the form of Eq. (17) only normal (tensile) forces are considered. The minimum number of spherical particles to represent for example a tensile specimen (at any size/scale) is two, as drawn in Fig. 18. Even when a macroscopic specimen is modelled in this way, the choice of two elements is allowed, but then of course the interaction potential must correspond to the measurement result. In this trivial case the input potential is exactly the same as the output potential, but the approach leads to problems since, for example, the effect of the rotation of the loaded boundaries of the tensile specimen (see in Van Mier 1997 for a detailed analysis of these effects) cannot be modelled using this minimal model. Structural effects must be modelled with models containing more spheres; for simulating the boundary rotation effects in tension, a minimum of two spheres over the width is essential. As an alternative, the two-body interaction should have angular stiffness.

7.5 Implications of using interaction potentials

As mentioned, a convenient environment to use $F-r$ potentials is lattice. The size of lattice elements

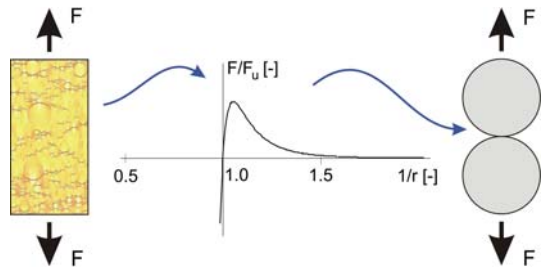

Fig. 18 Micro-mechanical analysis of a material specimen at a certain length scale L is used for determining the two-sphere $F-r$ interaction potential at the same size/scale

must resemble the scale of the material structure at the considered observational level. The potential function must be measured at the same level, and basically this means that experiments are needed from the atomic to the macroscopic scale levels. For fracture simulations, the stability of the lattice during the entire simulation from un-cracked to complete rupture is essential. Beam lattices are a simple and straightforward solution, and stability is guaranteed throughout the analysis. Another manner might be to consider three-particle interactions or higher, rather than two-particle interaction potentials, e.g., Stillinger and Weber (1985). As soon as more than two particles are used to represent the material, structural (construction) effects come into play. This basically means that behaviour found for a certain three-particle configuration cannot be directly transferred to other assemblages with, for instance, different angles between the three particles, different particle diameters, and/or different loading direction(s). It can also be the case that the particles have internal structure. Basically this is already the case at the atomic scale, and certainly also at larger scales.

The representation of fundamental material behaviour through an interaction potential as discussed above presumes that the particles at any size-scale cannot be divided, i.e., cannot be separated into smaller particles. This is an important restriction that has large implications for materials where the particles can actually break down in smaller parts. In practice this is possible, as was observed in the cement experiment of Fig. 9. In that example, the un-hydrated cement grains fracture, and can, as such, not take the function of a particle in the interaction potential. A better choice in

that case would be to go one size/scale down, i.e., to the level of the constituting cement clinker grains that can be seen, for instance, in Fig. 8 (i.e., the small grained internal structure of the whitish/light gray un-hydrated cement grains). Another option might be to include the particle rupture in the potential, which is acceptable as long as the break-up mechanism of the cement grains is considered in the construction of the potential function.

The two-particle interaction potential is to be considered as the most fundamental property of the material at a given scale. Structural effects cannot be simulated by means of two-particle interactions only, at least not in a central force lattice. Multi-particle interactions are essential for structural (construction) analysis, but they involve much more. For example frictional effects cannot be ignored, as depicted in Fig. 16b.[4] Two spherical particles are in contact through a single point only, and it is difficult to envision friction. However, a type of rolling friction may occur, at least if the boundary conditions of the spheres allow for rolling. This mechanism was included in a discrete element model by Iwashita and Oda (2000), and was found to have a significant effect on void formation in shear bands in loose granular media, as well as on the geometry of the shear-band at a larger scale. Thus, for friction the environment plays a significant role: rolling/sliding may occur in assemblages of spheres and global friction may be caused by jamming. This would suggest that friction is much more a global structural property, and not a material property, as would be favoured from a continuum mechanics point of view.

The idea of interaction potentials can be extended to compressive failure. A direct view of how this idea might work is given in Fig. 19. In contrast to sandstone, concrete contains particles of varying size (and often also, shape, but here we assume that all particles are spherical). Figure 19a shows the structure of sandstone, containing more-or-less equally sized sand grains bound together with, for example, clay or $CaCO_3$ (in Felser and Bentheimer sandstone, respectively). Under compressive load, the particle skeleton will transfer loads as sketched in Fig. 19b; contact between the particles is essential, and the behaviour of thin layers of clay in Felser sandstone will determine to a large extent how the interaction potential will look like. In the case of concrete a similar situation occurs, although there are some differences. Most important, particles have widely differing diameters as shown in Fig. 19c; after hydration of cement a situation emerges as drawn in Fig. 19d. The larger gravel grains are separated by zones of hydrated cement. The hydrated cement tends to have a larger porosity near the aggregates walls (in the ITZ, see also Sect. 2) and a smaller porosity at larger distances (in the so-called matrix, which also contains small sand grains). The behaviour of the cement layer between two grains of the particle skeleton in concrete will determine its compressibility; porosity decides the degree of compaction as was discussed by Bongers (1998). Detailed analysis of the cement layer behaviour in compression gives the correct interaction potential needed for computing the behaviour of the model in Fig. 19c.

The big question is whether the proposed multi-scale model can be successful or not. Ab-initio molecular dynamics is extremely time-consuming, and in the end the response of very small conglomerates of atoms can be calculated only using the largest available computers. It will be obvious that ab-initio analyses include all the structural conditions of the atoms directly, which remains rather problematic in any hierarchical (multi-scale) approach. In elasticity those problems can be overcome, but for fracture they appear un-solvable, unless as proposed in this Section *force–displacement (F-r) potentials* are used at all structural size/scale levels. The shape of the used potential is an issue, and there is a critical need for the right type of experiment to reveal these basic relations at various size/scale levels. At the macroscopic level the particles are not a reality, but rather a convenient representation of the material that allows for developing a multi-scale model. Lower scale processes are included in the interaction potential (next to mechanical, thermal and moisture related effects can be included conveniently as well), but in contradiction to the popular cohesive stress-

[4] The reader is reminded that quasi-static loading is considered here only. As soon as temporal effects become important, the interaction potential should be augmented to include said effects. In principle there are no constraints in doing this; the particle representation is quite suitable in this respect since it is relatively easy to model dynamics but also creep as an interface phenomenon.

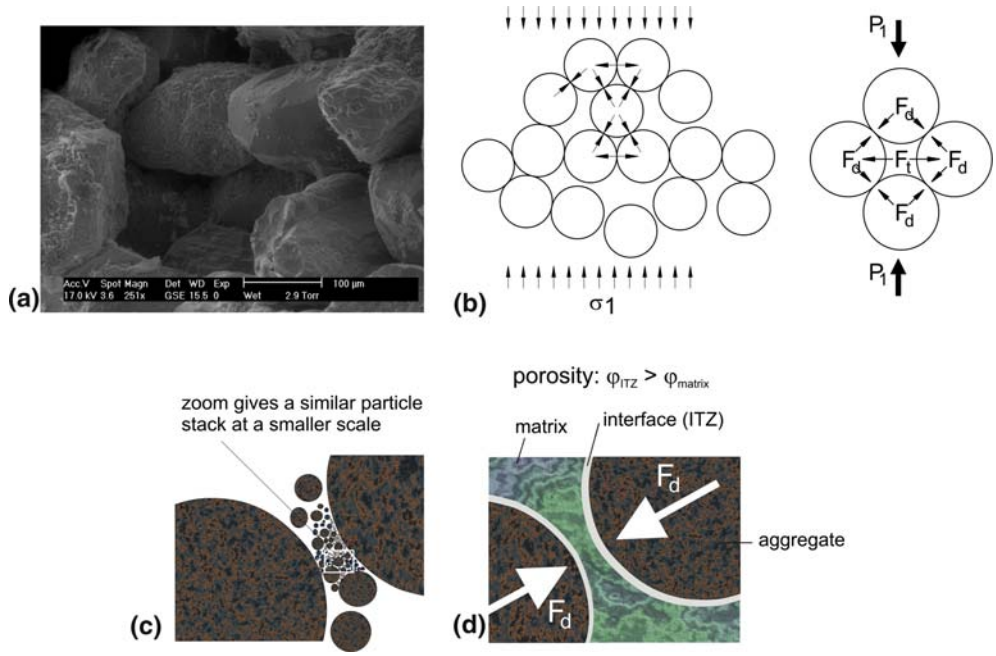

Fig. 19 Microstructure of sandstone; more-or-less equally sized sand grains are bound together by thin layers of clay or $CaCO_3$ (**a**); behaviour of a grain skeleton under external compression (**b**); particle structure of concrete contains many small cement and sand grains (**c**) that, after hydration, form a more-or-less continuous, but highly porous matrix between the larger gravel particles (**d**). The (compressive) interaction potential in the case of sandstone (**a**) would look different as the one for concrete (**d**) and depends on the local compatibility of the material between the grains. Water will play an important role in the case of Felser sandstone (clay binder!) porosity is very important in the case of concrete

crack-opening relation, one should resort to a *force–displacement relation*. Note that macroscopic models exist where the structure is represented by assemblages of spheres, e.g., Beranek and Hobbelman (1994). Their model is largely based on similarities with the lattice model presented in Sect. 3. Quite some work is needed to determine the correct interaction ($F - r$) potential, which in the work of Beranek and Hobbelman was assumed elastic-purely brittle like in the said lattice model. The multi-scale interaction potential in terms of force and displacement is an attempt to overcome difficulties imposed by the cohesive crack models where the growth aspect of macrocracking is missed, i.e., where structural influences are neglected ab initio.

8 Conclusion

The fracture behaviour of cement and concrete is complex owing to their heterogeneous material structure. As a result these materials show hardening, softening and localization of deformations under many—if not all—loading conditions such as uniaxial tension, uniaxial and multiaxial compression and extension. Only under very high confinement the material seems to behave truly plastic. Historically the fracture behaviour of these materials has always been treated in terms of continuum state variables stress and strain. In view of the localization of deformations in the direction of (external) loading, as well as the decreasing (intact) cross-sectional area during the softening regime, the use of both stress and strain as state variable appears to be rather debatable. In this paper the discussion is narrowed down to tensile loading. In practice it is not possible to determine size-independent softening parameters. The tensile strength, the shape of the softening curve, and the fracture energy, all depend to a lesser or larger degree on the structural environment of the experiment. The main obstacle seems the notion of stress,

as the last remnant of application of continuum theory in problems of localized fracture. Continuum theory is per definition based on averaging, and in fracture problems, in particular in the type of heterogeneous materials like cement and concrete (but also in related materials such as many types of rocks, ceramics, ice, clay and sand), the local loads and displacements between adjacent particles ultimately determine the onset and propagation of fracture. The geometry of the material structure plays an important role in all this, implying that a model must have strong footing in geometry.

In the paper, a simplified view is developed of the fracture behaviour of a material inside a structure. Microcracks caused by stress-concentrations in the heterogeneous material structure distinguish from macrocracks in the sense that they can be arrested by micro-structural elements inside the material structure, such as particles, fibre, pores, etc. Macrocracks are fatal cracks that can only be arrested or delayed by more rigorous structural measures that involve structural elements at much larger scale, or by changing the boundary and/or loading conditions (confinement). The growth of the macrocracks is to a large extent a structural phenomenon dictated mainly by loading conditions, specimen geometry and boundary conditions. As soon as macrocracking starts there is not much the material can do other than withstanding or delaying crack growth through bridging. In general in concrete and rock the effects on global softening are rather limited, except maybe for fibre reinforced concrete.

The main conclusion drawn in this paper is that the intertwinement of structural and material aspects should be eliminated for a fracture model to be successful. This is possible only when the material is thought to be constructed of elementary elements like spheres. An interaction potential describes the mechanical interaction between two spheres in contact. Two spheres is the bare minimum, and this configuration should be defined as the fundamental assembly for the determination of the interaction potential in terms of force and separation at the contact point. Given this principle, it would be logical to descend all the way down to the atomic level, but inherent problems in computation limit the size and time-span of analyses from that scale up tremendously. The solution must likely be found in a multi-scale potential, which describes the sphere interaction at various length scales.

Many issues have been raised in this paper, having in mind that fracture is quite similar under a large variety of loading conditions. Here point-wise some observations are given summarizing some of the most important issues.

(1) Hardening, softening and localization of deformations are salient characteristics of fracture of cement and concrete and related brittle disordered materials.
(2) The main influence of the material structure on the mechanical and fracture behaviour is in the hardening and bridging regimes.
(3) Under uniaxial tension hardening is usually neglected, or assumed not to exist. Yet, numerical simulations indicate that the specific build-up of the material may lead to a shorter or longer hardening regime. Significant hardening can be achieved in cementitious composites under tensile loading when fibres are added to arrest and bridge microcracks in very early stages of their growth.
(4) The hardening regime ultimately defines the strength of a material, and as such also scaling of strength and fracture energy. Cement and concrete show strong size/scale dependency, and basically none of the most common material parameters used in cohesive crack models, such as tensile strength and fracture energy, are scale-independent. These parameters can therefore not be considered as true material properties.
(5) Primitive models, like for example lattice, can be quite helpful in understanding details of the fracture process in disordered materials like cement and concrete. The essential outcome of such models is the fracture mechanism, which can be compared more easily to experimental results than stresses, which cannot be measured directly.

Since all parameters in cohesive crack models are size/scale dependant, improvement of these models in this respect is needed, in particular when prediction of failure of cement, concrete and other brittle disordered materials and structures in

hitherto not experimentally explored situations is asked for. An alternative might be to model the material based on multi-scale force-separation potentials ($F-r$) that describe the interaction between two neighbouring material elements. The potentials can be easily included in statistical fracture models like lattice, which can be applied at any size/scale.

9 New questions

The fracture behaviour of cement and concrete and brittle disordered materials in general is extremely complex. Many factors contribute, not only the heterogeneity of the material structure, but moisture and temperature distributions (during hydration) cause a constantly changing micro-structure, whereas temporal effects may lead to significant different response. In this paper the emphasis is on quasi-static loading, and the main interest is in understanding fracture and finding ways to model the observed behaviour. Many questions remain, such as:

(i) The actual strength distribution inside a disordered material is key-factor in developing a sound micromechanics-based model. For example in a 3-phase material strength and stiffness of the three-phases must be established. In particle models interaction potentials are required.

(ii) Crack detection techniques should be developed to show, possibly in three-dimensions, how (stable) microcracks nucleate and grow. An important aspect is to learn how those cracks are delayed and/or arrested in the material structure. This may give clues for modifying the material in order to achieve significant hardening response.

(iii) The material structure has smaller (in case of aggregate bridging) or larger (in case of fibre bridging) influence on the bridging stress. Understanding bridging is essential, especially when the goal is to improve the ductility of cement-based materials (both in tension and compression). For example, it has been found that when matrix material is reinforced with short fibres, the pull-out of long fibres from such a matrix can be significantly improved (see Markovic et al. 2003b).

(iv) The physical understanding of fracture scaling must be improved. It does not suffice to develop phenomenological models since extrapolation to un-explored size/scales is simply not possible. Understanding pre-critical cracking is a key-factor in understanding fracture scaling of strength.

(v) Interfaces between aggregate and cement play a key role in the fracture process of concrete; at smaller scales this may also be true for cement (see Figs. 10, 11). The popular way of modeling interfaces is by assuming a shell of interface material between aggregates and matrix. Close observation of material structures reveals that the ITZ cannot be regarded as an isotropic material with uniformly distributed porosity. The real image is far more complicated, which will certainly have an effect on micromechanical modeling.

(vi) Fracture mechanics of (partially) hydrated cement is considered as a challenging new area that deserves more attention, not in the least place because of the tremendous difficulties encountered in testing at such small scales. There are many parameters affecting the fracture behaviour of cement and better knowledge of the scaling behaviour of fracture of thin cement ribbons between adjacent aggregates in a concrete micro-structure, is essential for developing realistic micromechanical models for fracture. First insight in these matters suggests that softening may occur in cement if the dimension of the structure is sufficiently small.

(vii) Modelling cement and concrete and other disordered materials by means of force-separation interaction potentials ($F-r$) at various size/scale levels leads to many new questions, above all, whether this type of modeling is useful for circumventing computational problems that are met in ab-initio atomistic simulations. Size/scale dependency in a multi-scale interaction potential ($F-r$) model appears through the scaling of the ultimate contact force F_u in the potential; structural effects are included by considering multiple-particle systems ($N>2$), where the

case $N = 2$, the two-particle interaction is considered as the most fundamental interaction representing material behaviour.

Acknowledgements Several fruitful collaborations have been essential to the work underlying this paper. I am indebted to many of my former and present PhD students and colleagues (in alphabetical order): Jan Bisschop, Dino Chiaia, Chiara Corticelli, Allard Elgersma, Ahmed Elkadi, Erik van Geel, Giovanna Lilliu, Ivan Markovic, M.B. Nooru-Mohamed, Eduardo Prado, Silke Ruffing, Erik Schlangen, Tomoki Shiotani, Gerard Timmers, Pavel Trtik, Marcel van Vliet, Adri Vervuurt, Jeanette Visser and René Vonk.

References

Akita H, Koide H, Tomon M, Sohn D (2003) A practical method for uniaxial tension test of concrete. Mater Struct (RILEM) 36:365–371

Alava MJ, Nukala PKVV, Zapperi S (2006) Statistical models of fracture. Adv Phys 55(3–4):349–476

Arslan A, Schlangen E, Van Mier JGM (1995) Effect of model fracture law and porosity on tensile softening of concrete. In: Wittmann FH (ed) Fracture mechanics of concrete structures (FraMCoS-2). AEDIFICATIO Publishers, Freiburg, pp 45–54

Bazant MZ and Kaxiras E (1996) Modeling of covalent bonding in solids by inversion of cohesive energy curves. Phys Rev Lett 77(21):4370–4373

Bazant MZ, Kaxiras E, Justo JF (1997) Environment-dependent interatomic potential for bulk silicon. Phys Rev B 56(14):8542–8552

Bažant ZP and Cedolin L (1991) Stability of structures: elastic, inelastic, fracture and damage theories. Oxford University Press, New York

Bažant ZP (1984) Size effect in blunt fracture: concrete, rock, metal. J Eng Mech 110:518–535

Bažant ZP (1997) Scaling of quasi-brittle fracture: asymptotic analysis. Int J Fract 83(1):19–40

Bažant ZP, Tabarra MR, Kazemi MT and Pijaudier-Cabot G (1990) Random particle model for fracture of aggregate or fiber composites. J Eng Mech (ASCE) 106:1686–1705

Bentz DP (1997) Three dimensional computer simulation of Portland cement hydration and microstructure development. J Amer Ceramic Soc 80:3–21

Bentz DP, Quenard DA, Kunzel HM, Baruchel J, Peyrin F, Martys NS, Garboczi EJ (2000) Microstructure and transport properties of porous building materials. II: three-Dimensional X-Ray tomographic Studies. Mater Struct (RILEM) 33:147–153

Bentz DP, Coveney PV, Garboczi EJ, Kleyn MF, Stutzman PE (1994) Cellular automaton simulations of cement hydration and microstructure development. Model Simul Mater Sci Eng 2:783–808

Beranek WJ, Hobbelman GJ (1994) Constitutive modelling of structural concrete as an assemblage of spheres. In: Mang HA, Bicanic N, De Borst R (eds) Proceedings computational modelling of concrete structures (EURO-C). Balkema, Rotterdam, 412–426

Berlage ACJ (1987) Strength development of hardening concrete. PhD thesis, Delft University of Technology (in Dutch)

Berthelot J-M, Fatmi L (2004) Statistical investigation of the fracture behaviour of inhomogeneous materials in tension and three-point bending. Eng Fract Mech 71:1535–1556

Bisschop J (2002) Drying shrinkage microcracking in cement-based materials. PhD thesis, Delft University of Technology, Delft, The Netherlands

Bolander JE, Shiraishi T, Isogawa Y (1996) An adaptive procedure for fracture simulation in extensive lattice networks. Eng Fract Mech 54:325–334

Bongers H (1998) Multilevel analysis of concrete in multiaxial compression. In: De Borst R, Mang H, Bicanic N, Meschke G (eds) Computational modelling of concrete structures. Balkema, Rotterdam, 347–354

Breysse D (1991) Understanding some aspects of damage development using hierachic lattices. In: Van Mier JGM, Rots JG, Bakker A (eds) Fracture processes in concrete, rock and ceramics. Chapman & Hall, London/New York, 241–250

Burt NJ, Dougill JW (1977) Progressive failure in a model heterogeneous medium. J Eng Mech (ASCE) 103:365–376

Carpinteri A (1985) Interpretation of the Griffith instability as a bifurcation of the global equilibrium. In: Shah SP (ed) Proc NATO Adv Research Workshop on application of fracture mechanics to cementitious Composites, Evanston (IL) 1984. Martinus Nijhoff, Dordrecht, 287–316

Carpinteri A, Chiaia B, Cornetti P (2003) On the mechanics of quasi-brittle materials with a fractal microstructure. Eng Fract Mech 70:2321–2349

Carpinteri A, Chiaia B (1995) Multifractal nature of concrete fracture surfaces and size effects on nominal fracture energy. Mater Struct (RILEM) 28:435–443

Carpinteri A, Ferro G (1994) Size effects on tensile fracture properties: a unified explanation based on disorder and fractality of concrete microstructure. Mater Struct (RILEM) 27:563–571

Carpinteri A, Chiaia B, Ferro G (1995) Size effects on nominal tensile strength of concrete structures: multifractality of material ligaments and dimensional transition from order to disorder. Mater Struct (RILEM) 28:311–317

Carpinteri A, Chiaia B, Invernizi S (2004) Numerical analysis of indentation fracture in quasi-brittle materials. Eng Fract Mech 71:567–577

Célarié F, Prades S, Bonamy D, Ferrero L, Bouchaud E, Guillot C, Marlière C (2003) Glass breaks like metal, but at the nanometer scale. Phys Rev Lett 90(7):21 February 2003

Chiaia B, Vervuurt A, Van Mier JGM (1997) Lattice model evaluation of progressive failure in disordered particle composites. Eng Fract Mech 57:301–318

Colina H, Roux S (2000) Experimental model of cracking induced by drying shrinkage. Eur Phys J E 1:189–194

Constantinides G, Ulm FJ (2004) The effect of two types of C-S-H on the elasticity of cement-based materials: results from nanoindentation and micromechanical modeling. Cem Conc Res 34:67–70

Cundall PA and Strack ODL (1979) A discrete numerical model for granular assemblies. Géotechnique 29(1):47–65

D'Addetta GA (2004) Discrete models for cohesive frictional materials. PhD thesis, Stuttgart University, Germany

Diamond S (2000) Mercury Porosimetry—an inappropriate method for the measurement of pore size distributions in cement-based materials. Cem Conc Res 30:1517–1525

Diamond S, Huang J (1998) The interfacial transition zone: reality or myth? In: Katz A, Bentur A, Alexander MG, Arligue G (eds) Proc 2nd int'l conf on 'the interfacial transition zone in cementitious composites. RILEM Publications, Bagneux, 1–40

Donev A, Cisse I, Sachs D, Variano EA, Stillinger FH, Connelly R, Torquato S, Chaikin PM (2004) Improving the density of jammed disordered packings using ellipsoids. Science 303:990–993

Duxbury PM, Beale PD, Mourkazel C (1995) Breakdown of two-phase random resistor networks. Phys Rev B 51(6):3476–3488

Elfgren L (ed) (1989) Fracture mechanics of concrete structures—from theory to applications. Chapman & Hall, London/New York

Elkadi AS (2005) Fracture scaling of concrete under multiaxial compression. PhD thesis, Delft University of Technolgy

Elkadi AS, Van Mier JGM (2006) Experimental investigation of size effect in concrete fracture under multiaxial compression. Int J Fract 140:55–71

Elkadi AS, Van Mier JGM, Sluys LJ (2006) Multiaxial failure of low-cohesive frictional materials: fracture behaviour and size dependency. Phil Mag 86(21–22): 3137–3159

Evans RH, Marathe HS (1968) Microcracking and stress–strain curves for concrete in tension. Mater Struct (RILEM) 1:61–64

Foote RML, Mai Y-W, Cotterell B (1987) Crack growth resistance curves in strain-softening materials. J Mech Phys Solids 34:593–607

Gatty L, Bonnamy S, Feylessoufi A, Clinard C, Richard P, Van Damme H (2001) A transmission electron microscopy study of interfaces and matrix homogeneity in ultra-high-performance cement-based materials. J Mater Sci 36:4013–4026

Gmira A, Zabat M, Pellenq RJ-M, Van Damme H (2004) Microscopic physical basis of the poro-mechanical behaviour of cement-based materials. Mater Struct (RILEM) 37:3–14

Golterman P (1995) Mechanical predictions of concrete deterioration—Part 2: classification of crack patterns. ACI Mater J 92:58–63

Hansen A, Hinrichsen EL, Roux S (1991) Scale-invariant disorder in fracture and related breakdown phenomena. Phys Rev B 43(1):665–678

He M-Y, Hutchinson JW (1989) Crack deflection at an interface of dissimilar elastic materials. Int J Solids Struct 25:1053–1067

Herrmann HJ, Roux S (1990) Statistical models for the fracture of disordered media. North Holland, Amsterdam

Herrmann HJ, Hansen A, Roux S (1989) Fracture of disordered, elastic lattices in two dimensions. Phys Rev B 39(1):637–648

Heyden S (2000) Network modelling for the evaluation of mechanical properties of cellulose fibre fluff. PhD thesis, Lund University, Lund, Sweden

Hillerborg A, Modeer M, Petersson P-E (1976) Analysis of crack formation and crack growth in concrete by means of fracture mechanics and finite elements. Cem Conc Res 6:773–782

Holland D, Marder M (1999) Cracks and atoms. Adv Mater 11(10):793–806

Holzer L, Indutyi F, Gasser PH, Münch B, Wegmann M (2004) Three-dimensional analysis of porous BaTiO3 ceramics using FIB nanotomography. J Microscopy 216:84–95

Ince R, Arslan A, Karihaloo BL (2003) Lattice modelling of size effect in concrete strength. Eng Fract Mech 70:2307–2320

Iwashita K, Oda M (2000) Micro-deformation mechanism of shear banding process based on modified distinct element methods. Powder Techn 109:192–205

Jankovic D, Küntz M, Van Mier JGM (2001) Numerical analysis of moisture flow and concrete cracking in concrete by means of lattice type models, In: De Borst R, Mazars J, Pijaudier-Cabot G, Van Mier JGM (eds) Proceedings FraMCoS-IV. Balkema, Lisse/Abingdon/Exton/Tokyo, pp 231–238

Jennings HM (2000) A model for the microstructure of calcium silicate hydrate in cement paste. Cem Conc Res 30:101–116

Kalia R (2004) Hierarchical atomisitic simulations of fracture in nanostructured materials. In: Proceedings Lorentz workshop on satistical physics and pattern formation in fracture, Leiden, November 15–19 (CD-ROM)

Koenders EAB (1997) Simulation of volume changes in hardening cement-based materials. PhD thesis, Delft University of Technology.

Kotsovos MD (1983) Effect of testing techniques on the post-ultimate behaviour of concrete in compression. Mater Struct (RILEM) 16:3–12

Leung K-T, Néda Z (2000) Pattern formation and selection in quasistatic fracture. Phys Rev Lett 85(3):662–665

Lilliu G, Van Mier JGM (2003) 3D-lattice type fracture model for concrete. Eng Fract Mech 70:927–942

Lilliu G, Meda A, Shi C, Van Mier JGM (2002) Effect of particle density on tensile fracture properties of model concrete. In: Hendriks MAN, Rots JG (eds) Proceedings third DIANA World Conf. on 'finite elements in Civil Engineering Applications', Balkema, Lisse/Abingdon/Exton(PA)/Tokyo, 69–77

Lingen FJ (2000) Design of an object oriented finite element package for parallel computers. PhD thesis, Delft University of Technology

Maekawa K, Chaube R, Kishi T (1999) Modelling of concrete performance hydration. Microstructure Formation and Mass Transport, E&FN Spon, London

Markovic I, Van Mier JGM, Walraven JC (2003a) Development of high performance hybrid fibre concrete. In: Naaman AE, Reinhardt HW (eds) Proc. fourth int'l. RILEM workshop on 'High Performance Hybrid Fibre Concrete' (HPFRCC-4). RILEM Publications s.a.r.l., Bagneux, 277–300

Markovic I, Walraven JC, Van Mier JGM (2003b) Experimental evaluation of fibre pull-out from plain and fibre reinforced concrete. In: Naaman AE, Reinhardt HW (eds) Proc fourth Int'l. RILEM Workshop on 'High Performance Hybrid Fibre Concrete' (HPFRCC-4). RILEM Publications s.a.r.l., Bagneux, 419–436

Meakin P (1991) Simple models for material failure and deformation. In: Van Mier JGM, Rots JG, Bakker A (eds) Fracture processes in concrete, rocks and ceramics. E&FN Spon, London/New York, 213–229

Mourkazel C, Duxbury PM (1994) Failure of three-dimensional random composites. J Appl Phys 76(1):4086–4094

Mourkazel C, Herrmann HJ (1992) A vectorizable random lattice. J Stat Phys 68:911–923

Muguruma Y, Tanaka T, Tsuji Y (2000) Numerical simulation of particulate flow with liquid bridge between particles. Powder Techn 109:49–57

Nukala PKVV, Simunovic A (2005) Large-scale simulation of fracture networks. Proc 11th int conf of fract (ICF-11) Torino, Italy, March 20–25, 2005, 4097–4104 (CD-ROM).

Otsuka K, Date H, Kurita T (1998) Fracture process zone in concrete tension specimens by X-ray and AE techniques. In: Mihashi H, Rokugo K (eds) Fracture Mechanics of Concrete Structures—Proceedings FraMCoS-3. AEDIFICATIO Publishers, Freiburg, 1169–1182.

Pellenq RJ-M, Van Damme H (2004) Why does concrete set: the nature of cohesion forces in hardened cement-based materials. MRS Bull May 2004:319–323

Pignat C, Navi P, Scrivener K (2005) Simulation of cement paste microstructure hydration, pore space characterization and permeability determination. Mater Struct (RILEM) 38:459–466

Potyondy DA, Cundall PA (2004) A bonded-particle model for rock. Int J Rock Mech Min Sci 41:1329–1364

Prado EP, Van Mier JGM (2003) Effect of particle structure on mode I fracture process in concrete. Eng Fract Mech 70(14):1793–1807

Riera JD, Rocha MM (1991) On size effects and rupture of non-homogeneous materials. In: Van Mier JGM, Rots JG, Bakker A (eds) Fracture processes in concrete, rock and ceramics. Chapman & Hall, London/New York, 451–460

Roelfstra PE, Sadouki H, Wittmann FH (1985) Le béton numérique. Mater Struc (RILEM) 18:327–335

Sadouki H, Van Mier JGM (1996) Analysis of hygral induced crack growth in multiphase materials. HERON 41(4):267–286

Schärer R (2005) Micromechanical properties of Portland cements. MSc thesis, ETH Zurich, Department of Civil Engineering

Schlangen E (1993) Experimental and numerical analysis of fracture processes in concrete. PhD thesis, Delft University of Technology, The Netherlands

Schlangen E, Garboczi EJ (1997) Fracture simulations of concrete using lattice models: computational aspects. Eng Fract Mech 57(2/3):319–332

Schlangen E, Van Mier JGM (1992) Experimental and numerical analysis of the micro-mechanisms of fracture of cement-based composites. J Cem Conc Comp 14(2):105–118

Scrivener (1989) The microstructure of concrete. In: Skalny J (ed) Materials science of concrete—I. The American Ceramic Society, Columbus (OH), pp 127–161

Sempere J-C, Macdonald KC (1986) Overlapping spreading centers: implications from crack growth simulation by the displacement discontinuity method. Tectonics 5: 151–163

Shiotani T, Bisschop J, Van Mier JGM (2003) Temporal and spatial development of drying shrinkage cracking in cement-based materials. Eng Fract Mech 70(12):1509–1525

Simha KRY, Fourney WL, Barker DB, Dick RD (1986) Dynamic photoelastic investigation of two pressurized cracks approaching one another. Eng Fract Mech 23:237–249

Spooner DC, Pomeroy CD, Dougill JW (1976) Damage and energy dissipation in cement pastes in compression. Mag Conc Res 28(94):21–29

Stampanoni M, Borchert G, Wyss P, Abela R, Patterson B, Hunt S, Vermeulen D, and Ruegsegger P (2002) High resolution X-Ray detector for synchrotron-based microtomography. Nucl Inst Meth A491:291–301

Stankowski T (1990) Numerical simulation of progressive failure in particle composites. PhD thesis, University of Colorado, Boulder, USA

Steinbrech RW, Dickerson RM, Kleist G (1991) Characterization of the fracture behaviour of ceramics through analysis of crack propagation studies. In: Shah SP (ed) Toughening mechanisms in quasi-brittle materials. Kluwer Academic Publishers, pp 287–311

Stillinger FH, Weber ThA (1985) Computer simulation of local order in condensed phases of silicon. Phys Rev B 31(8):5262–5271

Stroeven M (1999) Discrete numerical modelling of composite materials. PhD thesis, Delft University of Technology, The Netherlands

Swanson PL, Fairbanks CL, Lawn BR, Mai, Y-W, Hockey BJ (1987) Crack interface grain bridging as a fracture resistance mechanism in ceramics: I. experimental study on alumina. J Am Ceram Soc 70(4):279–289

Taplin J (1959) A method for following the hydration reaction in Portland cement paste. Aust J Appl Sci 10: 329–345

Tennis PD, Jennings HM (2000) A model for two types of calcium silicate hydrate in the microstructure of Portland cement pastes. Cem Conc Res 30:855–863

Thortnton C, Antony SJ, (2000) Quasi-static shear deformation of a soft particle system. Powder Techn 109:179–191

Trtik P, Van Mier JGM, Stampanoni M (2005a) Three dimensional crack detection in hardened cement pastes using synchrotron-based computer micro-tomography (SRmCT) In: Proc 11th Int Conf of Fract (ICF-11) Symp 34 'Physics and Scaling in Fracture', Torino, Italy, March 20–25, pp 4470–4475 (CD-ROM)

Trtik P, Van Mier JGM, Landis EN, Stampanoni M, Stähli P (2005b) In-situ microtensile testing and 3D-imaging of hydrated Portland cement. Mater Struct (submitted)

Trunk B (2000) Einfluss der Bauteilgrösse auf die Bruchenergie von Beton. Building Materials Reports No. 11, AEDIFICATIO Publishers, ETH Zürich

Van Beugel K (1991) Simulation of hydration and formation of structure in hardening cement-based materials. PhD thesis, Delft University of Technology

Van Mier JGM (1984) Strain softening of concrete under multiaxial loading conditions. PhD thesis, Eindhoven University of Technology, The Netherlands

Van Mier JGM (1986) Multiaxial strain-softening of concrete. Mater Struct (RILEM) 19(111):179–200

Van Mier JGM (1991a) Mode I fracture of concrete: discontinuous crack growth and crack interface grain bridging. Cem Conc Res 21(1):1–15

Van Mier JGM (1991b) Crack face bridging in normal, high strength and lytag concrete. In: Van Mier JGM, Rots JG, Bakker A (eds) Fracture processes in concrete, rock and ceramics. Chapman & Hall, London/New York, pp 27–40

Van Mier JGM (1997) Fracture processes of concrete. CRC Press, Boca Raton (FL), 448 p

Van Mier JGM (2001) Micro-structural effects on fracture scaling in concrete, rock and ice. In: Dempsey JP, Shen HH (eds) Proc IUTAM symp on 'scaling laws on ice mechanics and ice dynamics'. Kluwer Academic Publishers, Dordrecht/Boston/London, pp 171–182

Van Mier JGM (2004) Lattice modelling of size effect in concrete strength. Discussion on a Paper by R. Ince, A. Arslan and B.L. Karihaloo. Eng Fract Mech 71(11): 1625–1628

Van Mier JGM, Chiaia BM, Vervuurt A (1997) Numerical simulation of chaotic and self-organizing damage in brittle disordered materials. Comp Meth Appl Mech Engng 142:189–201

Van Mier JGM, Shi C (2002) Stability issues in uniaxial tensile tests on brittle disordered materials. In: Proceedings IUTAM Symposium 'Material instabilities and the effect of micro-structure', Austin (TX) May 7–11, 2001. Int J Solids Struct 39(13/14):3359–3372

Van Mier JGM, Van Vliet MRA, Wang TK (2002) Fracture mechanisms in particle composites: statistical aspects in lattice type analysis. Mech Mater 34:705–724

Van Mier JGM, Van Vliet MRA (2003) Influence of microstructure of concrete on size/scale effects in tensile fracture. Eng Fract Mech 70(16):2281–2306

Van Mier JGM, Vervuurt A (1997) Numerical analysis of interface fracture in concrete using a lattice-type fracture model. Int J Damage Mech 6:408–432

Van Mier JGM, Vervuurt A, Schlangen E (1994) Boundary and size effects in uniaxial tensile tests: a numerical and experimental study. In: Bazant ZP, Bittnar Z, Jirdfsek M, Mazars J (eds) Fracture and damage of quasi-brittle structures. E&FN Spon, London/New York, 289–302

Van Vliet MRA (2000) Size effect in tensile fracture of concrete and rock. PhD thesis, Delft University of Technology, The Netherlands

Van Vliet MRA, Van Mier JGM (2000) Experimental investigation of size effect in concrete and sandstone under uniaxial tension. Eng Fract Mech 65(2/3): 165–188

Vervuurt A (1997) Interface fracture in concrete. PhD thesis, Delft University of Technology, The Netherlands

Visser JHM (1998) Hydraulically Driven Fracture of Concrete and Rock. PhD-thesis, Delft University of Technology

Vonk RA (1992) Softening of concrete loaded in compression. PhD thesis, Eindhoven University of Technology, The Netherlands

Vonk RA, Rutten HS, Van Mier JGM, Fijneman HJ (1991) Micromechanical simulation of concrete softening. In: Van Mier JGM, Rots JG, Bakker A (eds) Fracture processes in concrete, rock and ceramics. E & FN Spon, London/New York, pp 129–138

Wang J, Navi P, Huet C (1993) Finite element analysis of anchor bolt pull-out based on fracture mechanics. In: Rossmanith HP (ed) Fracture and damage of concrete and rock—FDCR2. E & FN Spon, London/New York, pp 559–568

Wissing B (1988) Acoustic emission of concrete. MS thesis, Dept of Civil Eng, Delft University of Technology (in Dutch)

Wittmann FH (1978) The cause and technological importance of capillary shrinkage of concrete. Betonwerk+Fertigteil Techn 5:272–276 (in German)

Ye G (2003) The Microstructure and Permeability of Cementitious Materials. PhD thesis, Delft University of Technology

Zech B, Wittmann FH (1978) A complex study on the reliability assessment of the containment of a PWR. Part II: probabilistic approach to describe the behaviour of materials. Nucl Engng Design 48: 575–584

Zimbelmann R (1985) A contribution to the problem of cement-aggregate bond. Cem Conc Res 15:801–808